

*Structure Prediction Of Clusters
Based On
The Exploration & Characterization
Of Their
Energy Landscapes*

Inauguraldissertation
zur

Erlangung der Würde eines Doktors der Philosophie
vorgelegt der
Philosophisch-Naturwissenschaftlichen Fakultät
der Universität Basel

von
Sandip De
aus Indien

Basel, 2012

Genehmigt von der Philosophisch-Naturwissenschaftlichen Fakultät auf
Antrag von:
Prof. Dr. Stefan Goedecker
Prof. Dr. D.G Kanhere
Basel, 22 May 2012

.
Prof. Dr. Martin Spiess

To My Parents

Abstract

The study of energy landscapes based on the electronic structure of materials is a fast growing field aided by the rapid advancements of both computational resources and the formulation of new efficient algorithms. Many properties of materials can now be determined directly from simulations based on electronic structure calculations. The study of energy landscapes is turning out to be the key of resolving many important problems in chemical physics and material science. In the field of innovation of new materials for technological advancement, computational structure prediction methods are becoming a time efficient and economical choice before taking decision of experimental synthesis. In this dissertation we present the application of a structure prediction method, Minima Hopping, to the exploration of energy landscapes of atomic clusters made of different elements. In addition to the reporting of several new stable clusters, the work goes beyond mere structure prediction, and answers several basic questions regarding the behavior of different clusters by studying their energy landscapes.

Contents

Abstract	5
Thank you	9
1 Introduction	11
1.1 Introduction	11
1.2 The Born-Oppenheimer approximation	11
1.3 Stationary points on PES	13
1.4 Features of Energy landscape	14
2 Global Optimization	19
2.1 Difficulties in finding global minimum	19
2.2 Overview on global optimization methods	22
2.2.1 Simulated Annealing	22
2.2.2 Basin Hopping Method	22
2.2.3 Genetic algorithms	23
2.2.4 Metadynamics	24
2.2.5 Minima Hopping Method	25
2.3 Comparison of Minima Hopping method with similar methods	26
3 The Effect Of Ionization On The Global Minima	35
3.1 Introduction	35
3.2 Methodology	36
3.3 Results	38

3.3.1	Silicon Clusters	38
3.3.2	Magnesium clusters	44
3.4	Conclusion	48
4	The Energy Landscapes Of Boron Clusters	55
4.1	Introduction	55
4.2	Small and Medium Size Boron Clusters	56
4.3	Chemical bonding in boron	62
4.4	Conclusion	64
5	Energy Landscapes Of Fullerene Materials	69
5.1	Introduction	69
5.2	Fullerene Cages	69
5.3	Boron Fullerene	71
5.4	Fullerenes in Nature	72
5.4.1	C_{60} Fullerenes	74
5.4.2	Boron-Nitride Fullerene	76
5.5	$C_{20}H_{20}$: A stable dodecahedrane found in nature	76
5.6	Comparison of energy landscapes	77
5.6.1	Fingerprint Vector	79
5.7	Cluster Interactions	81
5.8	Conclusion	84
6	Conclusions and Outlook	91
	List Of Publications	97
	Résumé	99

Thank You

It gives me a great pleasure to express my deep gratitude towards my supervisor, Prof. Stefan Goedecker for giving me the opportunity to work under him as a PhD student. I am thankful to him for his guidance, valuable advices and critical remarks regarding the scientific works. Constant encouragement and immense freedom from his side made the work environment productive yet very relaxing. Prof D.G. Kanhere was another source of support, encouragement and inspiration. I am thankful to him for providing valuable suggestions from time to time. I really appreciate the support from all the group members who helped maintaining a peaceful and productive work environment in the lab. Thanks to the secretaries of Department of Physics, Frau Kammermann and Frau Kalt for all their helps regarding official matters. Last but not the least the constant support from friends and family especially my parents always has been the key factor of all of my achievements.

I acknowledge the Indo-Swiss project grant for the financial support and Swiss National Supercomputing Centre (CSCS) for providing the computational resources.

1

Introduction

§1.1 Introduction

A potential energy surface is a mathematical function that gives the energy of a physical system as a function of its geometry. The structure of atomic and molecular clusters, the folding of proteins or the complex behavior of glasses have been successfully described in terms of potential energy surfaces (PES). In case of clusters and glasses the PES itself is often investigated directly, whereas for proteins and other biomolecules, it is also common to define free energy surfaces, which are expressed in terms of small number of order parameters.

The PES represents the potential energy of a given system as a function of all the relevant atomic or molecular coordinates. The potential energy V , for a system containing N atoms in three dimensions is a function of $3N$ -dimensional vector \vec{R} . The PES, $V(\vec{R})$, is therefore a $3N$ -dimensional object embedded in a $(3N + 1)$ -dimensional space. Our ability to focus upon $V(\vec{R})$, neglecting other degrees of freedom such as electronic coordinates relies on "Born-Oppenheimer approximation".

§1.2 The Born-Oppenheimer approximation

Any given physical system, can be described by a number of nuclei and electrons interacting through coulombic forces. We can write the Hamiltonian

of such a system in the following general form:[1]

$$\begin{aligned} \hat{H} = & - \sum_{I=1}^N \frac{\hbar^2}{2M_I} \nabla_I^2 - \sum_{i=1}^n \frac{\hbar^2}{2m} \nabla_i^2 + \frac{e^2}{2} \sum_{I=1}^N \sum_{J \neq I}^N \frac{Z_I Z_J}{|\vec{R}_I - \vec{R}_J|} \\ & + \frac{e^2}{2} \sum_{i=1}^n \sum_{j \neq i}^n \frac{1}{|\vec{r}_i - \vec{r}_j|} - e^2 \sum_{I=1}^N \sum_{i=1}^n \frac{Z_I}{|\vec{R}_I - \vec{r}_i|} \end{aligned} \quad (1.1)$$

Where $\vec{R} = \{R_I\}, I = 1, 2, \dots, N$ is a set of N nuclear coordinates, and $\vec{r} = \{\vec{r}_i\}, i = 1, 2, \dots, n$ is a set of n electronic coordinates. Z_I and M_I are the N nuclear charges and masses, respectively. All the ingredients are perfectly known and, in principle, all properties can be derived by solving the many body Schrödinger equation:

$$\hat{H}\Psi_i(\vec{r}, \vec{R}) = E_i\Psi_i(\vec{r}, \vec{R}) \quad (1.2)$$

In practice, however, the problem is almost impossible to treat in a full quantum mechanical framework. The full Schrödinger equation cannot be easily decoupled into a set of independent equations. So in general we have to deal with $(3N + 3n)$ coupled degrees of freedom. The usual practice is to use some sensible approximations.

The rest mass of electrons are much smaller than that of nucleus. Born and Oppenheimer argued that since a proton has a mass larger than a electron by a factor of 1836, so we can always assume that the nuclei stay in a stationary state when describing the electronic motion at any instant of time. In other words, the electron density should adjust almost instantaneously to changes in the positions of the nuclei. This is known as Born-Oppenheimer approximation. By applying this approximation we decouple the full wave function into two parts,

$$\Psi(\vec{R}, \vec{r}) = \psi_n(\vec{R})\psi_e(\vec{R}, \vec{r}) \quad (1.3)$$

Where $\psi_n(\vec{R})$ is the nuclear wave functions and $\psi_e(\vec{R}, \vec{r})$ is the solution of ‘electronic Hamiltonian’:

$$[\hat{H} - \hat{T}_n]\psi_e(\vec{R}, \vec{r}) = V_e(\vec{R})\psi_e(\vec{R}, \vec{r}) \quad (1.4)$$

Here \hat{H} denotes the total Hamiltonian operator in equation 1.1, and \hat{T}_n denotes the nuclear kinetic energy operator (the first term in equation 1.1).

$\psi_e(\vec{R}, \vec{r})$ is a function of electronic coordinate \vec{r} , but only depends upon the nuclear positions \vec{R} parametrically, because the above equation is solved for some particular nuclear geometry.

The potential energy surface defines the variation of the electronic energy, $V_e(\vec{R})$, with the nuclear geometry. It should be noted that different surfaces exist corresponding to different solutions of the equation 1.4 that represent excited electronic states.

§1.3 Stationary points on PES

The most interesting points of a potential energy surface are usually the stationary points where all the forces vanish, i.e. every component of the gradient vector is zero, $\partial V_e(\vec{R})/\partial R_\alpha = 0$ for $1 \leq \alpha \leq 3N$. From now on we will drop the 'e' subscript from V , which has been used until now to remind us that the PES describes the variation of the electronic energy with nuclear coordinates within the Born-Oppenheimer approximation. Since the forces vanish at such point the leading terms in the Taylor expansion of the potential are quadratic, and in normal coordinates [3]

$$V(\vec{Q}) = \frac{1}{2} \sum_{\alpha=1}^{3N} \omega_\alpha^2 Q_\alpha^2 + \mathcal{O}(Q^3),$$

Where $\vec{Q} = \vec{0}$ defines the stationary point and the zero of energy, and $\mathcal{O}(Q^3)$ denotes higher-order terms that are neglected in the harmonic approximation. The curvature which is the second derivative at $\vec{Q} = \vec{0}$ in the direction of a normal mode α is ω_α^2 . These parameters determine the local stability of a stationary point. A displacement along a normal coordinate α either raises or lowers the potential energy depending upon whether ω_α^2 is positive or negative. The characteristics of any stationary point are therefore determined by the Hessian eigenvalues, ω_α^2 at that point. Based on this discussion we can define three types of stationary points,

1. **Minima** : Minima are the stationary points with no negative Hessian eigenvalue. Any displacement results in an increase in the potential energy and a restoring force towards the minimum.
2. **First Order Saddle Point** : A first order saddle point or transition state is defined as a stationary point with a single negative Hessian

eigenvalue [2]. This negative eigenvalue also corresponds to a negative force constant or curvature and an imaginary normal mode frequency.

3. **Saddle Point of higher order:** A stationary point with more than one imaginary frequency is called higher order saddle point. A stationary point having k number of negative Hessian eigen values or k imaginary frequencies is called saddle point of order k . These points have a local maximum in k degrees of freedom.

§1.4 Features of Energy landscape

In the last section we have seen that the most important points in any PES are the stationary points. Depending on the presence of these stationary points, the features of PES can change arbitrarily from one system to another. Other than the stationary points defined in last section we will be using a few other terms to describe the PES.

1. **Basin :** A basin is, by the conventional definition, a certain part of the configurational space around a minimum of the potential energy surface. More precisely, a basin contains all the configurations that will relax into this minimum using simple small-step downhill relaxations. The union of several neighboring basin is called “super basin”.
2. **Funnel :** A funnel is defined as a super basin, in which one can arrive at the lowest minimum from any point of the super basin without crossing barriers that are very high compared to the average difference in energy between local minima.

Fig. 1.1 demonstrates an ideal energy landscape in order to clarify the definitions of the terms presented here. The clusters having high symmetry global minima, in general have a funnel like energy landscape in which finding the global minimum is easier than for glassy systems where the energy landscape consists of huge number of local minima in a small energy range.

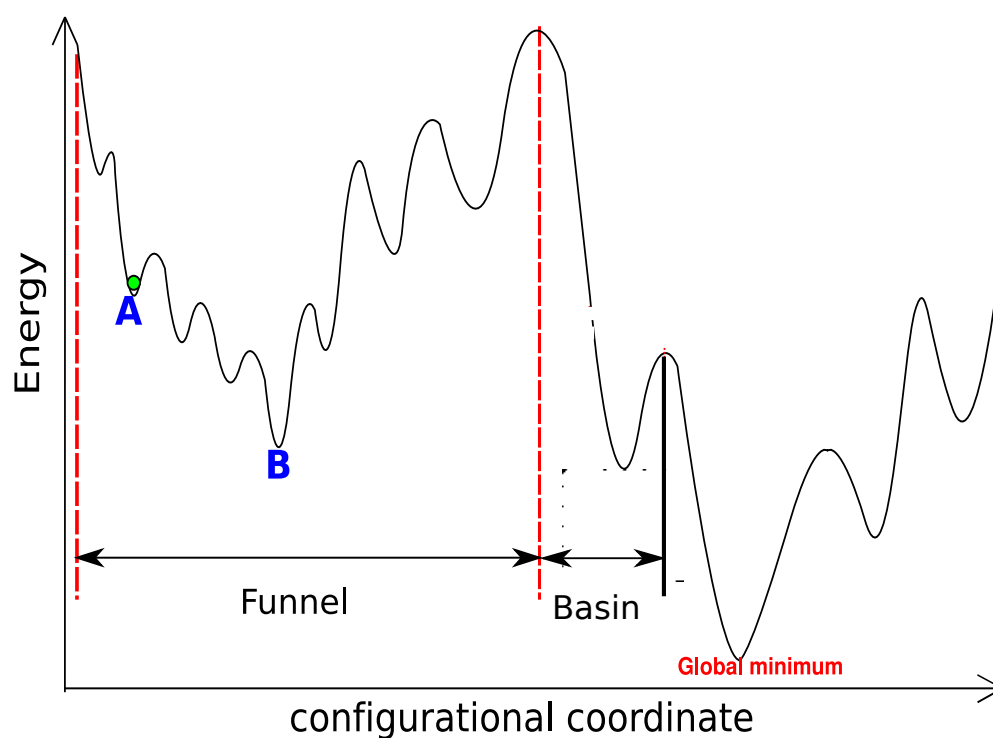


Figure 1.1: A model PES showing different features of a general energy landscape. Point (A) and (B) are local minima of the system. (B) is the lowest minimum for the funnel in the left. Note that to arrive at (B) from any point of the funnel such as minimum (A) one does not have to cross high barriers compared to the average difference in energy between local minima.

References

- [1] N. Giannopoulos, J. Kohanoff. *Density Functional Theory :Basics ,new trends and applications.* 2002.
- [2] J.N. Murrell and K.J. Laidler, *Trans Faraday Soc.* 64,371 (1968)
- [3] David Wales. *Energy Landscapes: Applications to Clusters, Biomolecules and Glasses (Cambridge Molecular Science).* Cambridge University press, 2003.

2

Global Optimization

A multidimensional PES has an enormous number of local minima and the low-lying energy configurations are the stable ones. In particular the lowest energy structure or global minimum corresponds to the most stable structure. Finding the global minimum is thus of great importance in physics, chemistry, and biology. The global minimum corresponds to:

- the crystalline structure of a periodic system
- the geometric ground state structure of a molecule or cluster
- the native state of a protein

Starting at a point in configurational space in order to find a minimum of PES, one uses minimization techniques such as steepest descent, conjugate gradient, etc. or sometimes combinations of them. There is no rigorous mathematical approach to find the global minimum or even to verify whether a given minimum is the global minimum or not. The only remedy to this problem at present is to consider the global minimum as the lowest energy minimum among many previously found local minima.

§2.1 Difficulties in finding global minimum

- **Huge number of local minima:** The fundamental difficulty associated with global optimizations is the exponential increase of the number of local minima with respect to the number of atoms in the system. For

example the molecules belonging to the hydro-carbon family (C_nH_{2n+2}) have number of local minima of the order of $\mathcal{O}(3^n)$. Due to this intrinsic problem, finding the global minimum for medium sized systems is already expensive and for larger systems might even be impossible with currently available resources.

- **Characteristics of energy landscape**

- The main difficulty in global optimizations arises in systems having several funnels, for the reason that the majority of the methods are deficient and in some cases incapable of finding the global minimum if the starting point is not in the funnel containing the global minima. For example the model energy landscape presented in fig. 2.1 contains two funnels. Now if one starts to explore the landscape starting from configuration (A), one will soon arrive at configuration (B), which is the lowest minimum for that funnel. But the global minimum of the system is in the other funnel, which is only accessible after crossing the high barrier between the two funnels. A systematic search algorithm will only try to cross the barrier after exploring a large number of local minima in the funnel, in which it starts in. Thus a good global optimization algorithm also needs to have the mechanism to climb up the high barrier to access the funnel containing global minimum. No random or systematic search algorithm will succeed in finding the ground state with 100% accuracy for an arbitrary energy landscape with an astronomically large number of local minima.
- The best type of energy landscape suitable for rapid exploration in order to find global minimum, is the one having a single funnel like feature. This type of energy landscape looks like the one presented in figure 2.2. Some examples of the systems having this kind of energy landscape are C_{60} , $B_{16}N_{16}$, $C_{20}H_{20}$ etc. In these cases one can generally obtain the global minimum rapidly using any kind of global minima search algorithm.

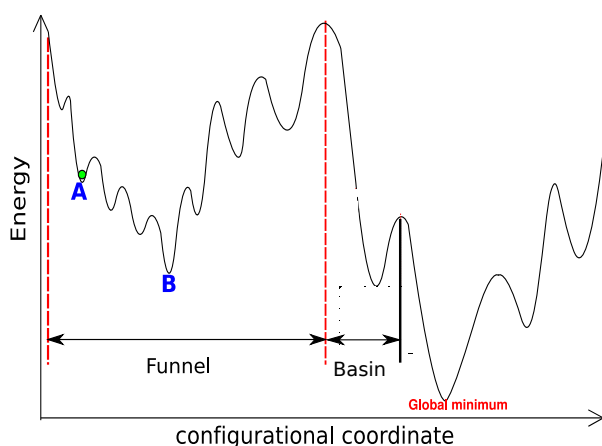


Figure 2.1: A multi-funnel energy landscape is very difficult to explore in order to find global minimum. Most of the clusters with exception of few have such energy landscapes. In these cases if one starts to explore the landscape from a configuration in the wrong funnel, any systematic algorithm will take a long time to get out of this funnel which does not contain global minimum.

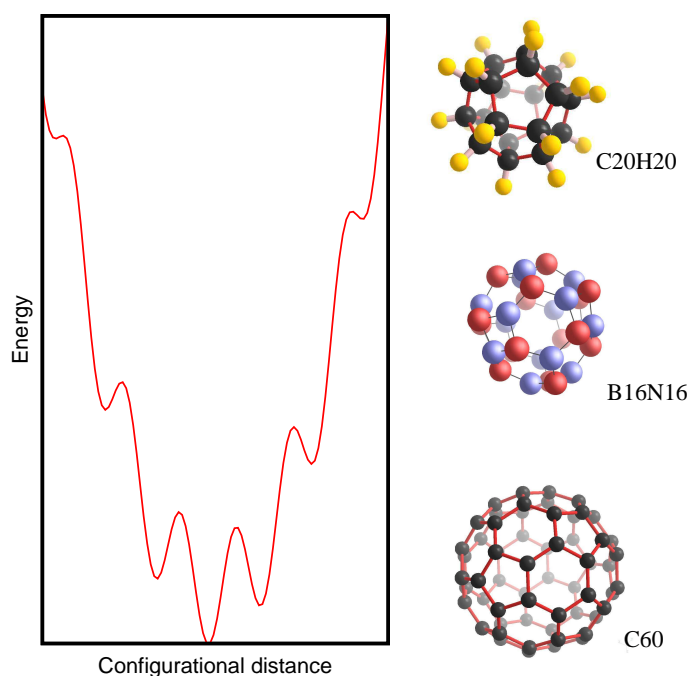


Figure 2.2: A single funnel energy landscape is easy to explore and finding global minimum is easier than in the case of a multi-funnel or featureless glassy landscape. C_{60} , $B_{16}N_{16}$ and $C_{20}H_{20}$ are the examples of systems having such energy landscapes.

§2.2 Overview on global optimization methods

There are plenty of the global optimization methods. In this dissertation we will only mention briefly the most successful ones.

▣2.2.1 Simulated Annealing

In real life, annealing is the process in which the temperature of a molten substance is slowly reduced until the material crystallizes to give a large single crystal. It is a technique that is widely used in many areas of manufacturing, such as the production of silicon crystals for computer chips. Simulated annealing [1, 2] is a computational method that mimics this process in order to find the global minimum. Initially at a given high temperature the system is allowed to reach approximately thermal equilibrium using a molecular dynamics or Monte Carlo simulations. At high temperatures, the system is able to sample high energy regions of configurational space and to pass over high energy barriers. As the temperature falls, lower energy configurations become more probable in accordance with the Boltzmann distribution. Eventually at very low temperature, the system is expected to occupy the lowest-energy configuration. This is however true only for systems with uncomplicated energy landscapes.

▣2.2.2 Basin Hopping Method

Basin Hopping (BHM) [3, 4] is a method in which the PES is mapped into a piece-wise constant function. This transformation associates any point in the configurational space with the local minimum obtained by a geometry minimization starting at that point,

$$\tilde{E}(\vec{R}) = \min\{E(\vec{R})\},$$

where \vec{R} represents the 3N-dimensional vector of the nuclear coordinates. In this transformation the transition state regions are effectively removed from the problem. Moreover, it does not change the global minimum, nor the relative energies of any local minima. The transformed energy landscape $\tilde{E}(\vec{R})$

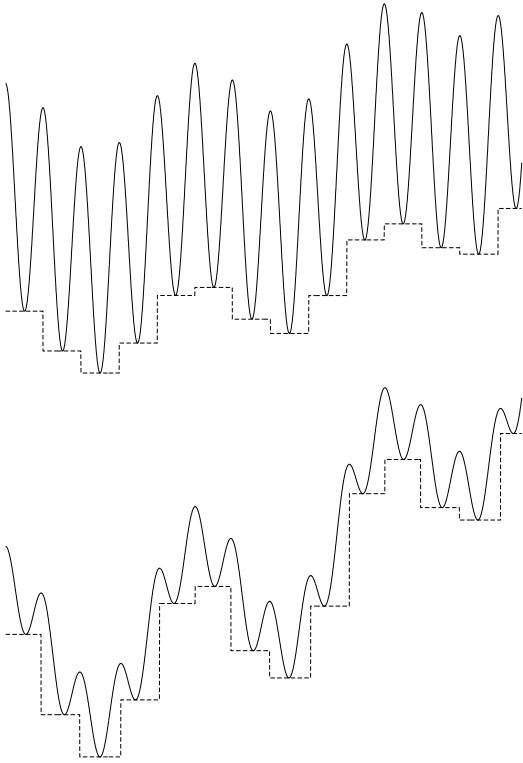


Figure 2.3: The effectiveness of the energy-landscape transformation in BHM strongly depends on the nature of the energy landscape. The figure in the upper panel indicates a situation, where the energy transformation indeed lowers the original high barriers whereas the figure in the lower panel indicates a situation where transformation did not improve the original situation much.

is then explored using a Monte Carlo simulation at a constant temperature. At each step, all coordinates are displaced by a random number in the range $[1, 1]$ times the step size, which is dynamically adjusted to give an acceptance ratio of 0.5.

The transformed piecewise constant potential energy surface of the basin hopping method still exhibits barriers that have to be overcome by Monte Carlo steps. If the height of these remaining barriers of the transformed surface between super-basins is small compared to the height of the original barriers of the untransformed surface between the basins (upper panel of Fig.2.3), the basin hopping method is expected to offer a significant advantage, otherwise (lower panel of Fig.2.3), the advantage will be marginal.

2.2.3 Genetic algorithms

Genetic algorithms [5, 6, 7, 8, 9] are a particular class of evolutionary algorithms and are among the most popular global optimization methods. They

were originally inspired by Darwins theory of evolution, more precisely they mimic the evolution processes in biology with inheritance and mutation from parents built into each new generation as the key elements. The first step in the implementation of any genetic algorithm is to generate an initial population of configurations, which is called the initial gene pool. In the next step one selects the gene candidates to create the next generation. The way to mix the selected genes of the two parents is called crossover, which reflects how the genetic attributes are passed on. Another effective way of exploring the PES in genetic algorithms is through the mutation process. In each of the three main operations (selection, crossover, mutation) in each generation, one makes sure that the configurations with the lowest energies always survive.

Genetic Algorithms have been applied to many other problems aside from global optimization for clusters, ranging from medical bioinformatics [10] to airframe design [11].

2.2.4 Metadynamics

Metadynamics [12, 13, 14] belongs to a class of methods in which sampling is facilitated by the introduction of an additional bias potential (or force) that acts on a selected number of degrees of freedom, often referred to as collective variables (CVs). A number of methods can be thought of as belonging to this class, such as umbrella sampling, [15] local elevation, [16] conformational flooding [17, 18] adaptive force bias, [19] steered MD, [20] and self-healing umbrella sampling. [21].

In metadynamics, an external history-dependent bias potential which is a function of the CVs is added to the Hamiltonian of the system. This potential can be written as a sum of Gaussians deposited along the system trajectory in the CVs space to discourage the system from revisiting configurations that have already been sampled. At the same time, metadynamics is able to enhance sampling and reconstruct the free-energy surface (FES) as a function of the chosen CVs. Although theoretically metadynamics has several strong points, the major difficulty of using it in practice is the choice of the CVs. Identifying a set of CVs appropriate for describing complex processes is far from trivial [12].

2.2.5 Minima Hopping Method

Unlike most of the other global optimization methods, which relies on thermodynamic principles, Minima Hopping Method (MHM) [22, 23] is a non-thermodynamic global optimization method. MHM aims at exploring the low energy part of the configurational space as fast as possible. The minima hopping method consists of an inner part that performs jumps into the local minimum of another basin and an outer part that will accept or reject this new local minimum. The acceptance/rejection is done by simple thresholding, i.e., the step is accepted if the energy of the new local minimum E_{new} rises by less than E_{diff} compared to the current energy E_{cur} . The parameter E_{diff} is continuously adjusted during the simulation in such a way that half of the moves are accepted and half are rejected. This outer part introduces a preference for steps that go down in energy. However if the inner part proposes only steps that go up in energy, such steps will finally also be accepted after E_{diff} has been sufficiently increased after many rejections.

A flowchart of the algorithm is given below. It contains five parameters. α_1 and α_2 determine how rapidly E_{diff} is increased or decreased in the case where a new configuration is rejected or accepted. β_1, β_2 , and β_3 determine how rapidly E_{kin} is modified depending on the outcome of an escape trial.

```

initialize a current minimum   Mcurrent
MDstart
ESCAPE TRIAL PART
start a MD trajectory with kinetic energy Ekinetic
from current minimum   Mcurrent . Once the
potential reaches the madmin-th minimum
along the trajectory stop MD and optimize
geometry to find the closest local minimum   M
if ( M   equals Mcurrent ) then
Ekinetic=Ekinetic!beta1 (beta1>1)
goto MDstart
else if ( M   equals a minimum visited previously)
then
Ekinetic=Ekinetic!beta2 (beta2>1)
goto MDstart
else if ( M   equals a new minimum) then
Ekinetic=Ekinetic!beta3 (beta3<1)
endif
DOWNWARD PREFERENCE PART

```

```

if (energy( M ) < energy( Mcurrent ) < Ediff) then
accept new minimum: Mcurrent = M
add Mcurrent to history list
Ediff=Ediff!alpha1 (alpha1<1)
else if rejected
Ediff=Ediff!alpha2 (alpha2>1)
endif
goto MDstart

```

Fig. 2.4 shows the possible escape moves from current local minimum within MHM. Each escape trial is followed by a local geometry relaxation. As indicated in the figure, If the new minimum is same as the old one or the $E_{new} - E_{current} > E_{diff}$, the move is rejected. when a new (unvisited) minimum is found, E_{kin} is multiplied by β_3 ($\beta_3 < 1$). Decreasing E_{kin} , whenever a new (unvisited) minimum is found, helps the simulation jump into another low energy basin by crossing low barriers. This is a very important feature of MHM because in this way the Bell-Evans-Polanyi (BEP) principle [24] is satisfied in an average sense. The BEP principle states that low energy molecular dynamics trajectories are more likely to cross into the basin of attraction of a low energy local minimum than high energy trajectories. [25]

In this dissertation we used MHM for our simulations. The systems considered in this study, have in most cases very complicated multi funnel energy landscape. To find the global minimum of such a potential energy surface requires an algorithm that can rapidly climb out of wrong funnels. This feature can only be obtained by abandoning the standard Markov-based Monte Carlo methods and by introducing a feedback mechanism that, based on the whole simulation history, enforces the exploration of new regions of the configuration space. The minima hopping method contains such a feedback mechanism.

§2.3 Comparison of Minima Hopping method with similar methods

The performance of MHM on several benchmark systems had already been addressed in detail before [22, 23]. In contrast to basin hopping, minima hopping is not a Monte Carlo method. What makes the significant difference in

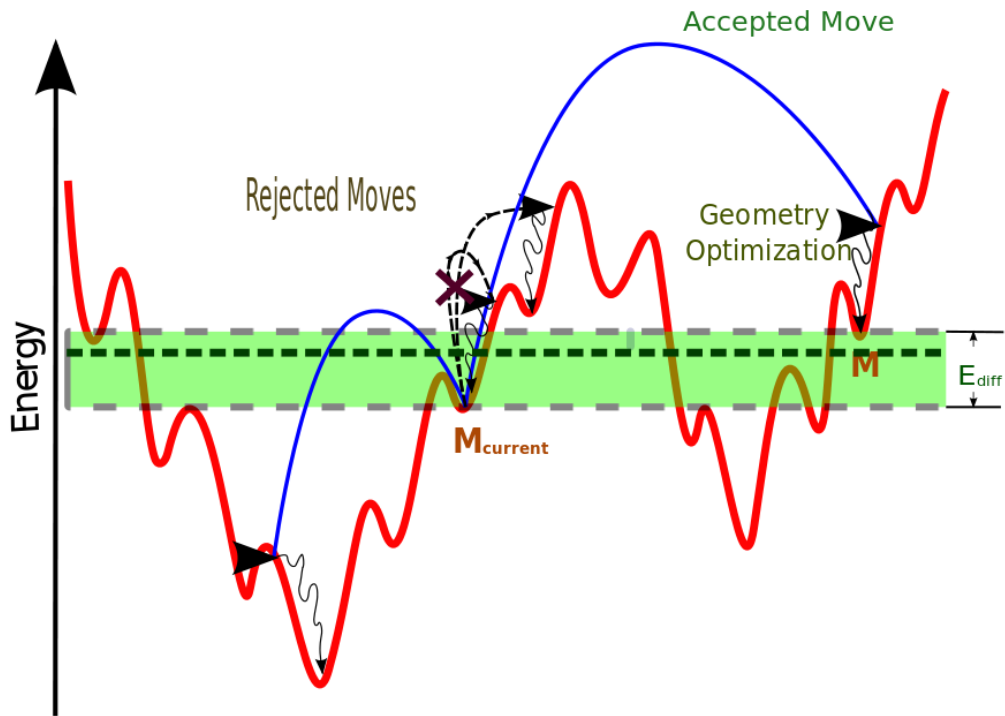


Figure 2.4: The Escape moves in Minima Hopping method. The black broken arrows indicate rejected moves and the unbroken blue ones represent allowed moves. The escape moves generally bring the system to a new basin. A local geometry relaxation then brings the system to a new local minimum. Addition to the favorable moves which brings the system to a lower energy local minimum, The moves which brings the system to a higher local minimum are also accepted if $E_{new} - E_{current} < E_{diff}$ condition is fulfilled. This option of accepting higher energy minima is the most important requirement to explore a multi-funnel energy landscape.

practice is the feedback introduced by the history list. As a consequence the minima hopping method can climb out of a wrong funnel much faster than the basin hopping method. It is thus superior to the basin hopping method for systems that have a deep wrong funnel. Wrong means in this context just that the funnel does not contain the global minimum. In Lennard-Jones benchmark systems it has been found that for the systems containing simple funnel like landscape, the performance of BHM and MHM are similar. For the systems containing two funnels such as the 38 atom Lennard-Jones cluster the performance of MHM was found better than BHM.

A detailed comparison of MHM with Genetic algorithms has also already been addressed [26]. The performance of Genetic algorithms (GA) is indeed better in case of systems having spherically symmetric global minima. Although it is in general not able to find global minima with geometrically difficult structures such as elongated silicon clusters and non-icosahedral ground states without the concept of niches. In contrast, minima hopping was able to find all ground states containing no symmetry.

A detailed performance comparison of MHM with other methods goes beyond the objectives of this dissertation. It is well understood that the performance of any global optimization algorithm strongly depends on the nature of the system and no algorithm can at present guarantee a 100% success rate. So rather than comparing with other methods, our objective was to use the algorithm to predict global minima of several different systems. MHM was very suitable for the kind of systems we were interested in. Below are the few points which made MHM a perfect tool for our purposes:

- In most of the cases the energy landscapes of the systems we explored were glassy in nature, ie they contained huge number of energetically closely spaced local minima and several funnels. As discussed before MHM can rapidly climb out the wrong funnel because of the feedback mechanism based of history list.
- The nature of the ground state in the systems we studied mostly did not have any well-defined structural motif. As discussed before, GA can be faster to predict spherical global minima than MHM but this nature of bias towards spherical global minima can result in failure in discovery of the global minima which have different structural motifs. For example Our study on B_{80} cluster predicted a configuration with no symmetry

as the global minimum in contrast to the previously widely accepted perfectly spherically symmetric fullerene structure. The UN-biasness of MHM made it ideal for using in all types of systems without doing any modification.

- Apart from the logical reasons discussed above, the main technical reason behind employing MHM for our purpose was a highly efficient implementation of MHM coupled with the BigDFT [27] code. We were interested to use DFT calculations instead of classical force field because DFT energy calculations are much more reliable than classical force fields. But DFT calculations are very expensive in nature even for modern super computers. To use global optimization directly on the DFT energy landscape, a very robust density functional program is required that can do hundreds of local geometry optimizations without failure. Many technical and algorithmic optimizations were performed [28] to combine MHM and Bigdft which allowed us to do our calculations accurately and efficiently.
- We constrained our focus only on clusters rather than periodic systems. Because of being wavelet based code, BigDFT [27] can handle isolated cluster system more easily than plane-wave based codes. In contrast to plane wave basis sets, free boundary conditions for charged systems are not problematic with a wavelet basis set. In plane wave program a neutralizing background charge is needed, since a periodic system can not have a charged unit cell. In a wavelet basis set the integral equation for the potential V

$$V(\mathbf{r}) = \int \frac{\rho(\mathbf{r}')}{|\mathbf{r} - \mathbf{r}'|} d\mathbf{r}'$$

can be solved directly for the electronic charge density ρ with a monopole and the electrostatic potential can therefore be calculated very accurately for charged systems [29].

References

- [1] S. Kirkpatrick, C. D. Gelatt, Jr., and M. P. Vecchi, *Science* 220, 671 (1983)
- [2] P. Salomon, P. Sibani and R. Frost, *Facts, Conjectures and Improvements for Simulated Annealing* SIAM, Philadelphia, 2002
- [3] D. J. Wales and J. P. K. Doye, *J. Phys. Chem. A* 101, 5111 (1997).
- [4] J. P. K. Doye and D. J. Wales, *Phys. Rev. Lett.* 80, 1357 (1998).
- [5] J. Mestres, G. E. Scuseria, *J. Comput. Chem.* 16, 729 (1995).
- [6] S. K. Gregurick, M. H. Alexander, and B. Hartke, *J. Chem. Phys.* 104, 2684 (1996).
- [7] J. A. Niesse and H. R. Mayne, *J. Chem. Phys.* 105, 4700 (1996).
- [8] D. M. Deaven and K. M. Ho, *Phys. Rev. Lett.* 75, 288 (1995).
- [9] D. M. Deaven, N. Tit, J. R. Morris, and K. M. Ho, *Chem. Phys. Lett.* 256, 195 (1996).
- [10] M.F Jefferson, et al *Cancer* 79, 1338 (1997)
- [11] David E Goldberg, *Genetic Algorithms in Search, Optimization, and Machine Learning* ,Addison-Wesley, Reading, MA (1989)

-
- [12] Alessandro Barducci, Massimiliano Bonomi, Michele Parrinello; *Metadynamics*, Wiley Interdisciplinary Reviews: Computational Molecular Science Volume 1, Issue 5, pages 826843, September/October 2011
- [13] Alessandro Laio and Francesco L Gervasio; *Metadynamics: a method to simulate rare events and reconstruct the free energy in biophysics, chemistry and material science 2008 Rep. Prog. Phys.* 71 126601
- [14] Laio A, Parrinello M. Escaping free energy minima. *Proc Natl Acad Sci USA* 2002, 99:1256212566.
- [15] Torrie GM, Valleau JP. Nonphysical sampling distribution in Monte-carlo free-energy estimation umbrella sampling. *J Comput Phys* 1977, 23:187 199
- [16] Huber T, Torda AE, Gunsteren WF. Local elevation: a method for improving the searching properties of molecular dynamics simulation. *J Comput-Aided Mol Des* 1994, 8:695708.
- [17] Grubmuller H. Predicting slow structural transitions in macromolecular systems: conformational flooding. *Phys Rev E* 1995, 52:28932906.
- [18] Muller EM, de Meijere A, Grubmuller H. Predicting unimolecular chemical reactions: chemical flooding. *J Chem Phys* 2002, 116:897905.
- [19] Darve E, Pohorille A. Calculating free energies using average force. *J Chem Phys* 2001, 115:91699183.
- [20] Park S, Schulten K. Calculating potentials of mean force from steered molecular dynamics simulations. *J Chem Phys* 2004, 120:59465961.
- [21] Marsili S, Barducci A, Chelli R, Procacci P, Schettino V. Self-healing umbrella sampling: a nonequilibrium approach for quantitative free energy calculations. *J Phys Chem B* 2006, 110:1401114013.
- [22] Stefan Goedecker; *Minima hopping: An efficient search method for the global minimum of the potential energy surface of complex molecular systems*, JOURNAL OF CHEMICAL PHYSICS VOLUME 120, NUMBER 21 (2004)
- [23] Maximilian Amsler and Stefan Goedecker: Crystal structure prediction using the minima hopping method, *J. Chem. Phys.* 133, 224104 (2010)

-
- [24] F. Jensen, Computational Chemistry Wiley, New York, 1999
- [25] Shantanu Roy, Stefan Goedecker, and Vladimir Hellmann; Bell-Evans-Polanyi principle for molecular dynamics trajectories and its implications for global optimization, Phys. Rev. E 77, 056707 (2008)
- [26] Sandro E. Schnborn, Stefan Goedecker, Shantanu Roy and Artem R. Oganov, The performance of minima hopping and evolutionary algorithms for cluster structure prediction, J. Chem. Phys. 130, 144108 (2009)
- [27] Luigi Genovese, Alexey Neelov, Stefan Goedecker, Thierry Deutsch, Seyed Alireza Ghasemi, Alexander Willand, Damien Caliste, Oded Zilberberg, Mark Rayson, Anders Bergman, and Reinhold Schneider. Daubechies wavelets as a basis set for density functional pseudopotential calculations. *The Journal of Chemical Physics*, 129(1):014109, 2008.
- [28] Global Minimum Determination of the Born-Oppenheimer Surface within Density Functional Theory Stefan Goedecker, Waldemar Hellmann, and Thomas Lenosky Phys. Rev. Lett. 95, 055501 (2005)
- [29] Luigi Genovese, Thierry Deutsch, Alexey Neelov, Stefan Goedecker, and Gregory Beylkin. Efficient solution of poisson's equation with free boundary conditions. *The Journal of Chemical Physics*, 125(7):074105, 2006.

The Effect Of Ionization On The Global Minima

§3.1 Introduction

Since experimental mass selection methods require ionized systems, the majority of experimental information on clusters was obtained for ionized clusters. On the other hand, neutral systems are of greater practical interest and the majority of theoretical works are done on neutral systems. The relation between the properties of neutral and ionized clusters is therefore an important one. The basic property which determines all other properties is the structure. Finding the global minimum structure of a cluster is a complex global geometry optimization problem on a high dimensional potential energy landscape [1] with a huge number of local minima. In order to make accurate structural predictions, the potential energy surface should be calculated within density functional theory. Doing exhaustive unbiased searches for the global minimum at the density functional level has only recently become possible through the combined improvements in global optimization algorithms and computer performance.

One basic question concerning the relation between neutral and ionized clusters is whether they have the same basic structure. Evidently adding or removing one electron will change the the exact bond lengths and angles but one might suspect that the structures remain nevertheless very similar. The relation between the structure of neutral and ionized clusters has been investi-

gated in numerous previous publications for the same silicon and magnesium clusters that we have reexamined. The conclusion, in all the publications we are aware of, is that in general the structures of the neutral and cation clusters are more or less identical, but the criteria for being ‘identical’ are not always explicitly given. We introduce a well defined criterion for being identical. Two minima are identical or more precisely ‘related’, if the equilibrium structure of the ionized system lies within the catchment basin of the neutral system and vice versa. Applying this criterion on an extensive database of accurately relaxed geometries, we arrive at the opposite conclusion.

§3.2 Methodology

The global and local minima presented here are obtained within Density functional theory using the ‘Big DFT’ wavelet code [11] which was coupled to the ‘minima hopping’ [10] global optimization algorithm. The local spin density approximation (LDA) is used together with HGH type pseudo potentials [4] for the calculation of the potential energy surface. The size of the wavelet basis set was chosen such that the energies were converged to within better than 10^{-4} Hartree with respect to the infinite size basis set. A combination of conjugate gradient and BFGS methods [5] was used for the local geometry optimizations and they were stopped when the numerical noise in the forces was about 20 percent of the total force. This happened usually when the largest force acting on any atom was less than 2×10^{-5} Hartree/Bohr. Saddle points were found by a modified version of the ‘A spline for your saddle’ method [6].

In contrast to plane wave basis sets, free boundary conditions for charged systems are not problematic with a wavelet basis set. In plane wave program a neutralizing background charge is needed, since a periodic system can not have a charged unit cell. In a wavelet basis set the integral equation for the potential V

$$V(\mathbf{r}) = \int \frac{\rho(\mathbf{r}')}{|\mathbf{r} - \mathbf{r}'|} d\mathbf{r}'$$

can be solved directly for the electronic charge density ρ with a monopole and the electrostatic potential can therefore be calculated very accurately for charged systems [7].

For all the clusters we have carried out separate global optimization runs for neutral and ionized system. Since anions with weakly bound additional electrons are less accurately described by density functional theory than cations, we considered only cations in addition to the neutral system. For small clusters (less than 10 atoms for silicon and less than 20 atoms for magnesium) the majority of low energy local minima can be obtained. That this condition is fulfilled can be deduced in the minima hopping algorithm from a strong increase in the kinetic energy of the molecular dynamics trajectories. For larger clusters this explosion of the kinetic energy [8] can not be observed for any reasonable short simulation time. In case of medium sized clusters we calculated always at least 100 low energy local minima structures and we did various empirical checks to convince ourselves that the global minimum was found. We checked for instance always that the lowest energy structures found for the cation system did not relax upon addition of an electron into a structure that was lower in energy than the putative global minimum found for the neutral system.

Using this approach we investigate whether the global minimum structures of neutral and positively charged clusters are related. We will use the following two criteria as the definition for two structures of a neutral and ionized system to be “related”

- The equilibrium structure i of the cation will relax into the equilibrium structure j of the neutral cluster when an electron is added.
- The equilibrium structure j of the neutral cluster will relax into the equilibrium structure i of the cation when an electron is removed.

By relaxations we mean local geometry optimization with a sufficiently small step size, which will make it very unlikely that the local geometry optimization jumps out of the catchment basin within which the local geometry optimization was started. The structures of the neutral and ionized system are thus considered to be related, if there is a one-to-one mapping between the global minima structures upon addition and removal of an electron. This definition of two structures being related is motivated by the fact that the removal or addition of an electron in an experiment is quasi instantaneous on the time scale of the motion of the heavy nuclei. A cluster will therefore relax experimentally into the minimum of the catchment basin in which it

finds itself after the addition or removal of an electron.

In order to see whether our definition is fulfilled or not, we have introduced mapping charts that show which local minimum of the neutral system relaxes into which local minimum of the ionized system and vice versa. We consider the global minima structures of the neutral and ionized cluster to be identical if the two global minima structures are related according to the above definition.

In order to detect the degree of similarity between two structures with N_{at} atoms and atomic coordinates R^a and R^b respectively we have also calculated the configurational distance D

$$D = \frac{1}{N_{at}} \sqrt{\sum_{i=1}^{3N_{at}} (\mathbf{R}_i^a - \mathbf{R}_i^b)^2}$$

The two structure were rotated and shifted in such a way as to minimize D . In addition atomic numbers were permutated in the search for the smallest possible D . It turns out that structures, that are related according to our definition, usually have also a small configurational distance, but the opposite is not true.

We have chosen silicon and magnesium clusters for this study since they are among the most extensively studied clusters and since we wanted to see whether clusters made out of insulating and metallic materials behave in the same way.

The figures are produced using 'v_sim' (http://inac.cea.fr/L_Sim/V_Sim/index.en.html). The symmetry group was found using vmd [9] plug-ins [10].

§3.3 Results

▣3.3.1 Silicon Clusters

For silicon system we did our calculation for small clusters containing 3 -19 atoms and for Si_{32} as an representative of medium size clusters. For very small clusters there exist only a few local minima structures and they are therefore usually well separated in energy. As the number of atoms in the cluster grows, the number of meta-stable structures increases exponentially.

The concept of a global minimum is already rather ill-defined for silicon clusters containing more than some 7 atoms. They have many quite distinct structures that are very close in energy to the global minimum structure [11]. As a consequence more than one structure can be populated even at room temperature. A second consequence of this is that different density functionals can give a different energetic ordering of the various minima [12] and even with the most accurate Quantum Monte Carlo calculations it is difficult to obtain the resolution necessary to predict the correct energetic ordering [11]. In this study we are not claiming to identify the correct ground state structures of the studied silicon clusters, but instead we want to show general trends. Therefore we use standard density functional theory instead of the extremely expensive Quantum Monte Carlo method. Considering the fact that completely different structures can be extremely close in energy suggests strongly that a major perturbation such as the addition or removal of an electron can change the energetic ordering of the structures. Older studies have in contrast frequently just assumed that the ground state structures of neutral and positively charged clusters are the same. In some more recent investigations, few cases were identified where the neutral and positively charged cluster were not ‘related’. In an investigation, where silicon clusters with less than 20 atoms were investigated [13], Si_8 , Si_{12} , Si_{13} , Si_{15} and Si_{17} were found as the exceptions where the ground state geometries of the cation differ from the one of the neutrals. In another investigation of silicon clusters with less than 10 atoms [14], the ground state geometry of Si_9 and Si_{10} were found to be the “related”. Both studies are in contradiction to our results which show that for silicon clusters with more than 7 atoms, the ground state structures of the neutrals and cations are not related with the only exception of Si_9 and Si_{18} and are as a matter of fact quite different (Fig. 3.1). In another study of medium sized clusters [15] it was also found that in most cases the structures of the neutrals and cations are the same. Out of the medium size clusters we have only examined the 32 atom cluster for which we however also find different ground state structures.

Fig: 3.2 and Fig: 3.3 shows the mapping chart which gives detailed information about the relaxation properties upon addition and removal of an electron . We distinguish between reversible and irreversible mappings between pairs of local minima. The energies of all the structures are measured with respect to the ground state energy of the neutral system. Solid double

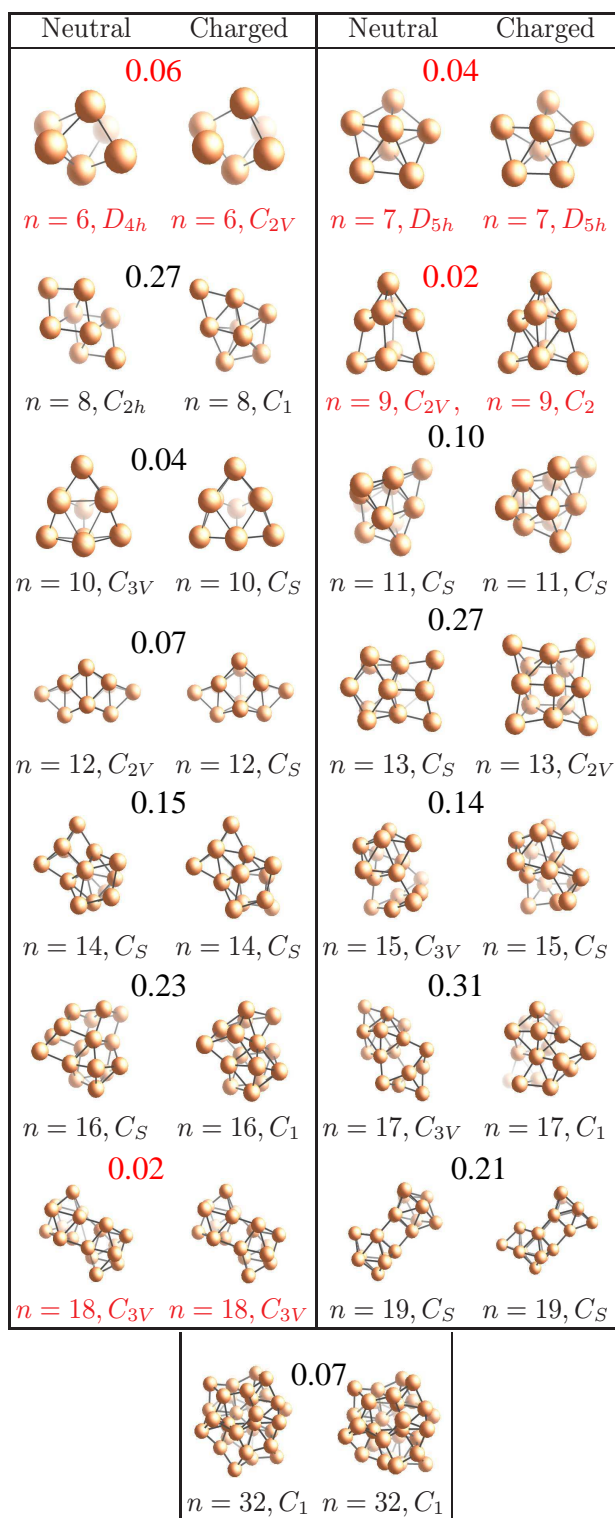


Figure 3.1: Global minima of charged and neutral Si_n , for $n=6,7,\dots,19$ and 32. Only for $n=6,7,9$ and 18 the global minima of charged and neutral are “related”. The configurational distance between each pair is given in Å.

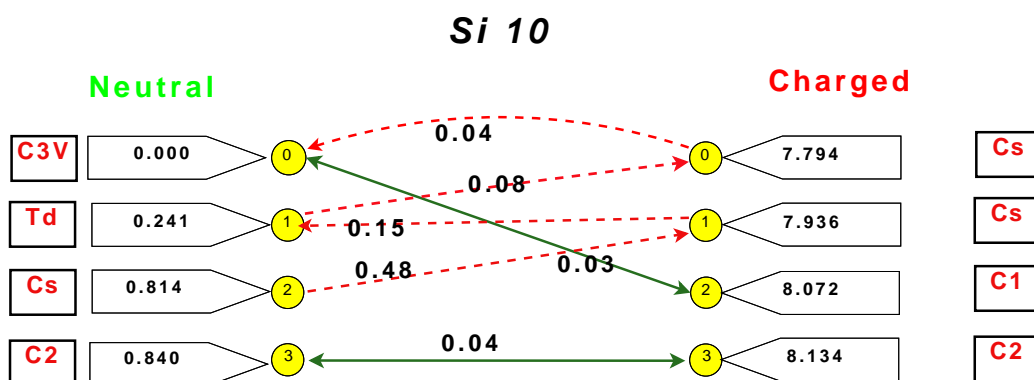


Figure 3.2: Mapping chart for Si_{10} . The configurational distance between the neutral and charged ground state configurations is very small (0.04 Å) and ionized ground state does relax into the neutral ground state when an electron is added. However the neutral ground state does not relax into the ionized ground state and therefore the structures are not ‘related’ according to our definition. This behavior is rather exceptional and was only found for Si_{10} , Si_{12} , Mg_{25} and Mg_{56} . For all the other unrelated structures neither the ionized ground state relaxes into the neutral ground state nor the neutral into the ionized one.

arrow connecting lines denote reversible mappings and dashed single arrow connecting line irreversible mappings. The space group is given in the rectangular boxes and the numbers close to the the connecting lines give the configurational distance of the two configurations.

A reversible mapping connects two structures which are related according to our definition. In an irreversible mapping, the cluster relaxes from the i -th to the j -th local minimum when an electron is removed or added, but it relaxes to a structure which is different form the i -th when the electron is given back or taken away again. Fig: 3.2 and Fig: 3.3 shows that both kinds of mappings are encountered frequently. The minima of the neutral and cation are related according to our aforementioned definition only if a reversible mapping connects the two global minima. This case was never encountered for clusters of more than 7 atoms except for Si_9 and Si_{18} and the global minimum structures for the neutrals and cations are thus different except for Si_n $n=3$ to 7 , 9 and 18 in this size range . The numerical values along the relaxation arrows in the mapping diagrams indicate the configurational distances in the relaxation processes. These distances are typically of the order of 0.03 Å, and thus show that the distortion during the relaxation is rather small. The symmetry group is also conserved in most cases. The fact that the geometries change so little upon removal or addition of an electron might have contributed to the wrong believe that the ground state of the neutral and cation are more or less identical. Nevertheless these small displacements are frequently sufficient to bring the system in another catchment basin.

The energetic ordering for neutral and ionized cluster configurations would be identical if the ionization energy or electron affinities (including the energy that comes from the small relaxation upon removal or addition of an electron) would be constant, i.e. independent of the shape of the various meta-stable configurations. The essential point is however that ionization energies and electron affinities are about two orders of magnitude larger than the energy differences between the ground state structure and the next meta-stable low energy structures. Relatively small differences in the ionization energies and electron affinities between the different configurations can therefore lead to a reversal of the energetic ordering of the local minima. The energy differences between the ground state and the first meta-stable configuration is of the order of few $k_B T$ at room temperature and the energy differences between the higher meta-stable configurations are even smaller.

We find small configurational distance values not only for the structural changes induced by the addition or removal of an electron but also between different local minima of the neutral and ionized clusters. The configurational distance between the first and second meta-stable configuration of the Si_{14} cluster is for instance only 0.15 Å. Nevertheless the two local minima are separated by a barrier of about 1.2 eV. In these disordered structure a broad distribution of barrier heights is to be expected [28] and we find indeed also low barriers. The configurational distance between the ground state of the charged Si_{10} cluster and its first meta-stable configuration is for instance also 0.15 Å. But the barrier between the two structures are much smaller namely 0.22 eV and 0.08 eV respectively. Such small barrier heights are well below the accuracy level of density functional methods and it can hence not be excluded that higher level calculations such as coupled cluster or Quantum Monte Carlo calculation would give a different potential energy surface. Our previous experience [17] shows however that barrier height are quite well reproduced by density functional theory if no bonds are broken during the transformation from one structure to the other.

3.3.2 Magnesium clusters

For Mg_n we have systematically studied all small and medium size clusters with $n=6$ to 30 atoms as well as Mg_{56} . The Global minima are shown in Fig. 3.4.

For these cluster sizes the electronic HOMO-LUMO gap does not yet tend to zero, but is around 0.1 eV. So no pronounced metallic behavior is present. The ionization energies are also comparable to the case of the silicon clusters. The ionization energy is on average 5 eV for the magnesium clusters and 7eV for the silicon clusters. The only notable difference we found between the silicon and magnesium cluster is number of meta-stable states, which is much larger for silicon clusters. Since all energy differences are however also smaller for Mg than for Si , the average configurational distance between different meta-stable configurations is again similar in both cases. Hence Mg clusters have the same overall behavior as the Si clusters, i.e in general the neutral and ionized ground states are not related.

In the studied size range we find that the global minima of neutral and cation clusters are related for $n=7,8,12,15,17,18,19,24,26,27,30$ and 32. For a bigger system, Mg_{56} we also found the global minima to be different for charged and neutral system. So in total the ground state structures are related in 12 cases and unrelated in 21 cases. Fig. 3.5 and Fig. 3.6 exemplifies the same kind of mapping for Mg_{16} and Mg_{24} between charged and neutral system as we already showed for silicon systems. These mapping charts look very similar to that of silicon systems, i.e. the energetic ordering changes when the system goes from the neutral to the charged state. Although for Mg_{24} the neutral and charged global minima are ‘related’, from the mapping chart (Fig. 3.6) we can see the sign of energetic ordering changes in the system while going from neutral to charged state. The numerical values along the relaxation arrows in the mapping diagrams indicate the configurational distances in the relaxation processes. These distances are typically of the order of 0.02 Å, unlike Silicon systems where this value is 0.03 Å, and thus show that the distortion during the relaxation is smaller than that of silicon systems.

Our results are again overall in disagreement with the majority of previous publications. In one of the earliest publication on this topic, where clusters with up to 6 atoms were studied, identical ground state structures were found for Mg_6 and Mg_7 [18]. In a study of Mg cluster with up to 21 atoms, it was found that only for Mg_3 and Mg_4 the ground states are different [19]. In another somewhat more extensive study in the range between 2 and 22 atoms [20], it was found that in addition also Mg_6 , Mg_7 , Mg_8 , Mg_{11} , Mg_{12} and Mg_{13} have different ground states.

We have also recalculated the energetic ordering of the minima of several magnesium clusters with the PBE functional [21]. In all these cases the ordering was identical to the ordering with the LSD functional. This is in contrast to the silicon clusters where the energetic ordering depends on the functional being used. This suggests that the density functional results for the magnesium clusters are very reliable.

For the magnesium clusters the average configurational distance between the various local minima is typically in the range between 0.1 Å, and 0.2 Å, and thus larger than the average configurational distance of the relaxation

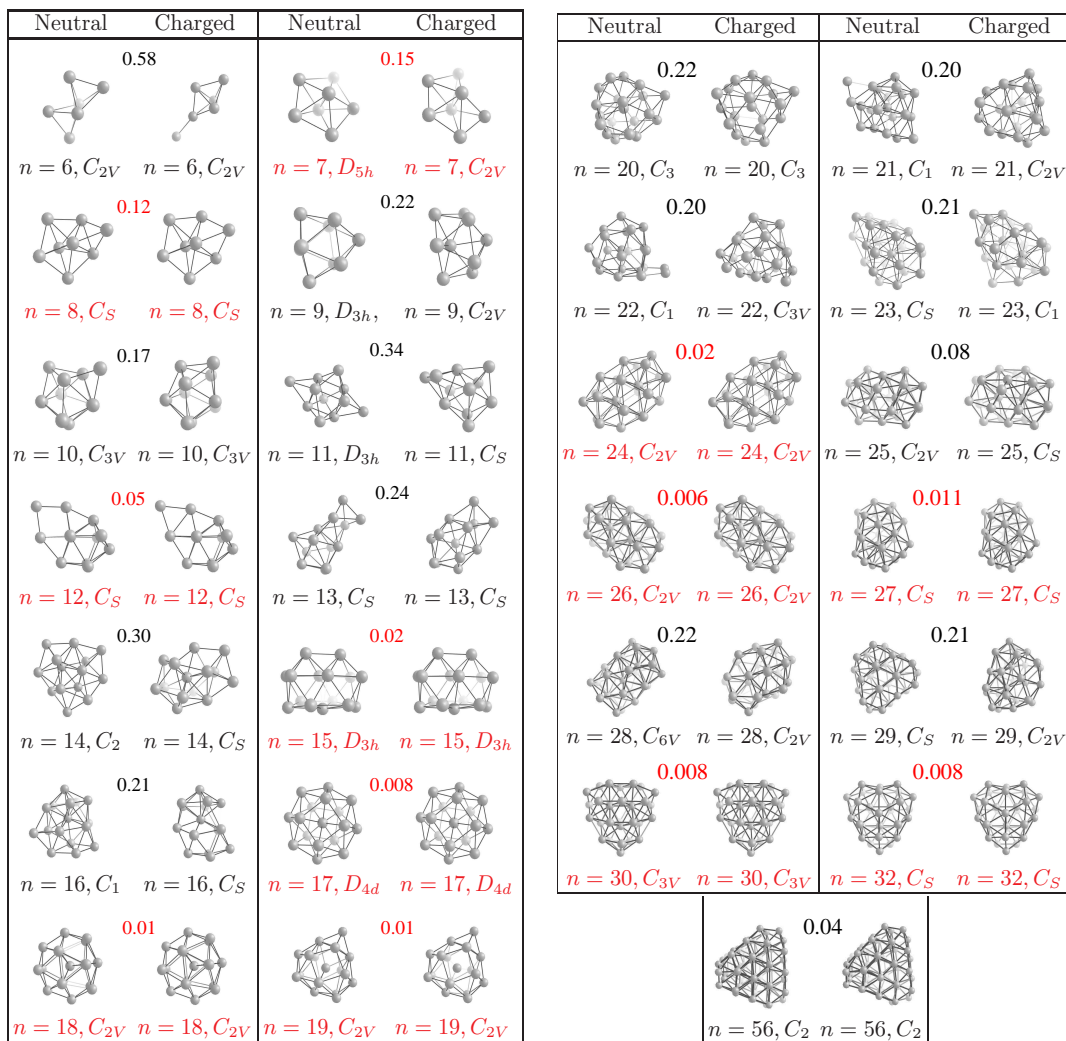


Figure 3.4: Global minima of charged and neutral Mg_n , for $n=6-30,32,56$. Only for $n=7,8,12,15,17,18,19,24,26,27,30$ and 32 the global minima of charged and neutral are “related”. The configurational distance between each pair is given in Å

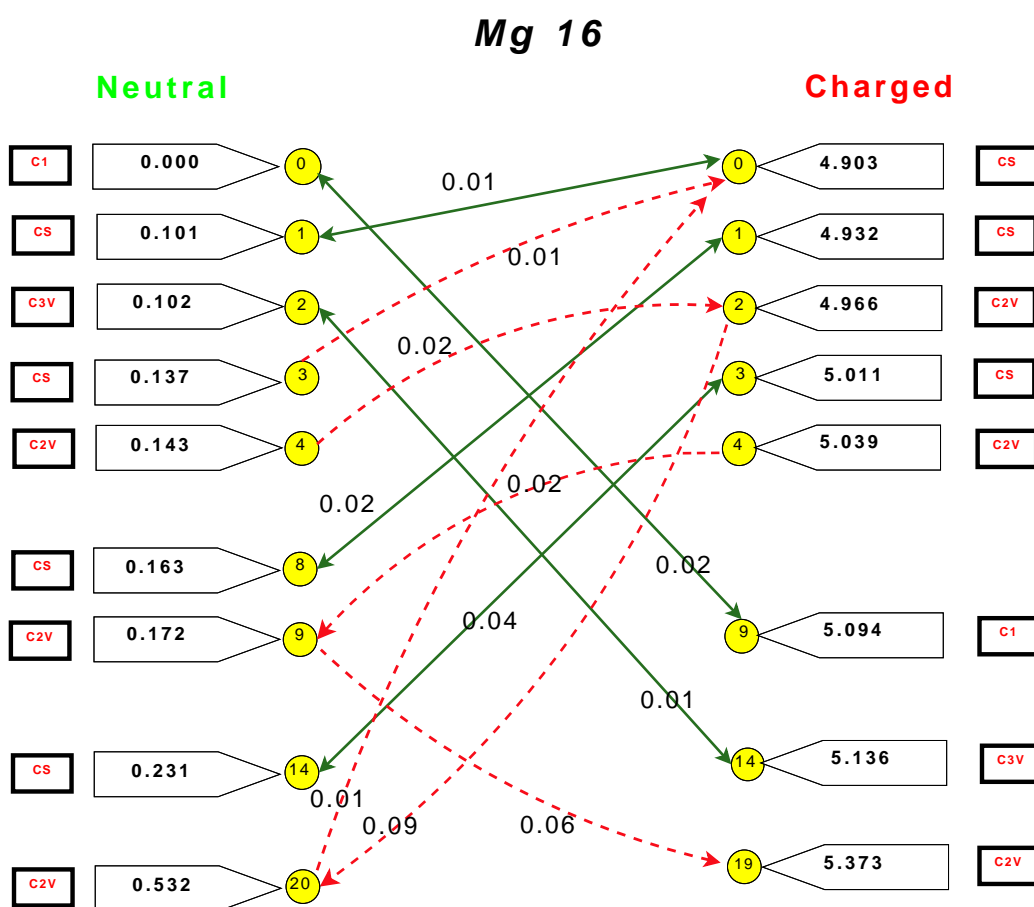


Figure 3.5: Mapping chart for Mg_{16} . The ground state of the neutral cluster is mapped to a rather high local minimum of the charged cluster.

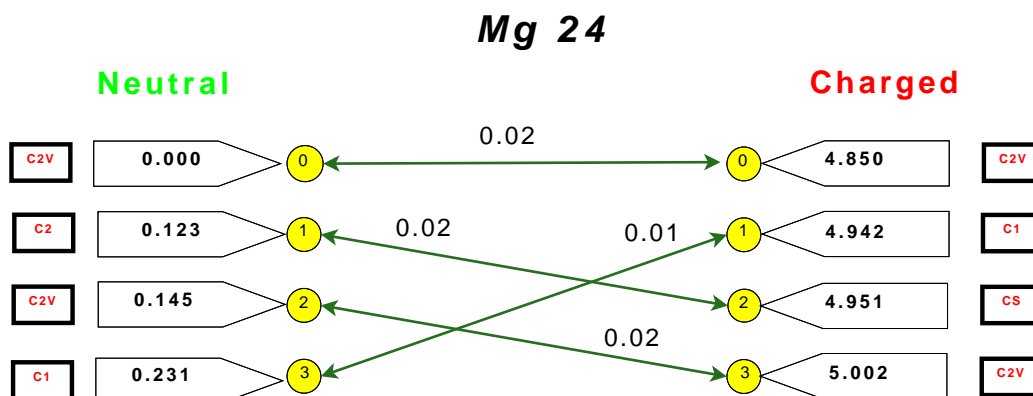


Figure 3.6: Mapping chart for Mg_{24} . For this system the ground states are related. The higher energy meta-stable states are however even for such a system typically not ‘related’.

induced the the removal or addition of electrons. Since the magnesium cluster are also disordered we find, as in the case of the silicon clusters, a broad distribution of barrier heights. We calculated randomly 12 barrier heights of the neutral Mg_{16} and Mg_{24} cluster and we found values in between 0.05 and 0.8 eV.

§3.4 Conclusion

Using an exhaustive sampling of the low energy configurations based on the minima hopping method we show for silicon and magnesium clusters that the ground states of neutral and ionized clusters are in general not related and are in many cases quite different. This comes from the fact that for medium and large clusters there are in general numerous meta-stable structures which are energetically very close to the ground state. The differences in ionization energies and electron affinities for different structures are much larger than this energy difference between structures. These facts have to be taken into account in the interpretation of experiments with ionized clusters.

There is no reason to believe that clusters made out of other elements behave differently. Based on our arguments one can only expect that for certain magic cluster sizes, for which ground state structures exist that are considerably lower in energy than other competing meta-stable structures,

the ground state does not change upon removal or addition of an electron. Such an example is for instance the C_{60} fullerene.

References

- [1] David Wales. *Energy Landscapes: Applications to Clusters, Biomolecules and Glasses (Cambridge Molecular Science)*. Cambridge University Press, 2003.
- [2] Luigi Genovese, Alexey Neelov, Stefan Goedecker, Thierry Deutsch, Seyed Alireza Ghasemi, Alexander Willand, Damien Caliste, Oded Zilberberg, Mark Rayson, Anders Bergman, and Reinhold Schneider. Daubechies wavelets as a basis set for density functional pseudopotential calculations. *The Journal of Chemical Physics*, 129(1):014109, 2008.
- [3] Stefan Goedecker. Minima hopping: An efficient search method for the global minimum of the potential energy surface of complex molecular systems. *The Journal of Chemical Physics*, 120(21):9911–9917, 2004.
- [4] C. Hartwigsen, S. Goedecker, and J. Hutter. Relativistic separable dual-space gaussian pseudopotentials from h to rn. *Phys. Rev. B*, 58(7):3641–3662, Aug 1998.
- [5] Jorge Nocedal. Updating quasi-newton matrices with limited storage. *Mathematics of Computation*, 35(151):pp. 773–782, 1980.
- [6] Rebecca Granot and Roi Baer. A spline for your saddle. *The Journal of Chemical Physics*, 128(18):184111, 2008.
- [7] Luigi Genovese, Thierry Deutsch, Alexey Neelov, Stefan Goedecker, and Gregory Beylkin. Efficient solution of poisson’s equation with free

- boundary conditions. *The Journal of Chemical Physics*, 125(7):074105, 2006.
- [8] Stefan Goedecker. *published in Modern Methods of Crystal Structure Prediction, Edited by Artem R. Oganov*. Wiley-VCH, 2011.
- [9] William Humphrey, Andrew Dalke, and Klaus Schulten. VMD – Visual Molecular Dynamics. *Journal of Molecular Graphics*, 14:33–38, 1996.
- [10] John Stone, Justin Gullingsrud, Paul Grayson, and Klaus Schulten. A system for interactive molecular dynamics simulation. In John F. Hughes and Carlo H. Séquin, editors, *2001 ACM Symposium on Interactive 3D Graphics*, pages 191–194, New York, 2001. ACM SIGGRAPH.
- [11] Waldemar Hellmann, R. G. Hennig, Stefan Goedecker, C. J. Umrigar, Bernard Delley, and T. Lenosky. Questioning the existence of a unique ground-state structure for si clusters. *Phys. Rev. B*, 75(8):085411, Feb 2007.
- [12] Soohaeng Yoo and X. C. Zeng. Structures and relative stability of medium-sized silicon clusters. iv. motif-based low-lying clusters si₂₁–si₃₀. *The Journal of Chemical Physics*, 124(5):054304, 2006.
- [13] Liu Bei. ; Lu Zhong-Yi ; Pan Bicaï ; Wang Cai-Zhuang ; Ho Kai-Ming ; Shvartsburg Alexandre A ; Jarrold Martin F. Ionization of medium-sized silicon clusters and the geometries of the cations. *Jcp*, 109(21):9401–9409, 1998.
- [14] Xu-yan Zhou Li Bao-xing, Pei-lin Cao. Electronic and geometric structures of sin and sin+ (n = 210). *phys. stat. sol. (b)*, 2003.
- [15] R. L. Zhou and B. C. Pan. Low-lying isomers of si_n⁺ and si_n⁻ (n = 31–50) clusters. *The Journal of Chemical Physics*, 128(23):234302, 2008.
- [16] A. Heuer, *Journal of Physics: Condensed Matter* 20, 373101 (2008) ; G. Daldoss, O. Pilla, G. Viliiani, C. Brangian and G. Ruocco, *Phys. Rev. B* **60** 3200 (1999)
- [17] S. Alireza Ghasemi, Maximilian Amsler, Richard G. Hennig, Shantanu Roy, Stefan Goedecker, C. J. Umrigar, Luigi Genovese, Thomas

-
- J. Lenosky, Tetsuya Morishita, Kengo Nishio: *Phys. Rev. B* 81, 214107 (2010)
- [18] F. Reuse, S. N. Khanna, V. de Coulon, and J. Buttet. Behavior of magnesium clusters under electron attachment and detachment. *Phys. Rev. B*, 39(17):12911–12914, Jun 1989.
- [19] Andrey Lyalin, Ilia A. Solov'yov, Andrey V. Solov'yov, and Walter Greiner. Evolution of the electronic and ionic structure of mg clusters with increase in cluster size. *Phys. Rev. A*, 67(6):063203, Jun 2003.
- [20] Julius Jellinek and Paulo H. Acioli. Magnesium clusters: structural and electronic properties and the size-induced nonmetal-to-metal transition. *The Journal of Physical Chemistry A*, 106(45):10919–10925, 2002.
- [21] John P. Perdew, Kieron Burke, and Matthias Ernzerhof. Generalized gradient approximation made simple. *Phys. Rev. Lett.*, 77(18):3865–3868, Oct 1996.

4

The Energy Landscapes Of Boron Clusters

§4.1 Introduction

Relative to its next-door neighbor carbon, boron is one electron short. And that makes a huge difference in chemical bonding and properties among each other.

Carbon, with six electrons, is essential to life, while boron, with only five, is not. There are countless organic compounds having innumerable uses, but there are many fewer examples of boranes (the boron analogs of hydrocarbons) and their carborane and metallaborane derivatives. The number of applications for these boron compounds in electronics, catalysis, organic synthesis, and diagnostic and therapeutic medicine, while growing, has been limited. Nevertheless, because boron is different, with a diverse set of structural and bonding characteristics, chemists have remained fascinated with the prospects of discovering new families of functional boron compounds, particularly all-boron clusters.

To explore the energy landscape of the boron clusters we do global geometry optimizations on the density functional potential energy surface with the minima hopping algorithm [10]. All the density functional calculations are done with the BigDFT electronic structure code [11] which uses a systematic wavelet basis together with pseudopotentials [12] and the standard LDA [12] and PBE [13] exchange correlation functionals.

§4.2 Small and Medium Size Boron Clusters

We explored the energy landscape of few small and medium size boron clusters, for $n=12,14,16,17,18,19,21,22,24,32,33,34$ and 36 in order to find the global minimum of the system. We also extensively studied the energy landscape of B_{80} to observe several interesting features which lead to formulation of a methodology to comment on the feasibility of experimental synthesis of a proposed nano-structure. The details will be discussed in the next chapter.

The global minimum structures of boron clusters are presented in Fig. 4.1. It is interesting to note that up to $n = 19$ Boron clusters prefer to form planar structures. Upto $n = 18$ the structures are consist of only filled hexagons. From $n = 19$ we can see both filled pentagon and hexagons. In this size range the clusters show a strong tendency to form cages and all the numerous low energy structures we found are cage like. This is agreement with a recent study [16] where the ground state was found to be cage like.

These medium size clusters contain well known structural motifs [17] namely empty and filled hexagons as well as empty and filled pentagons. But in addition they contain numerous other structural motifs such as single atoms connecting filled hexagons or rings containing more than 6 atoms. The inclusion of these other structural motifs does not increase the energy significantly and the first meta-stable structure is typically only 0.1 eV higher in energy than the global minimum. For B_{32} we found for instance some 100 cage like isomers in an energy interval of only 1 eV above the global minimum and even more isomers presumably exist in this interval. The number of nearest neighbors in these structures varies from 4 to 6 and the bond angles vary from 90 degrees for some 4 fold coordinated corner atoms to 60 degrees for 6 fold coordinated atoms in the center of a planar hexagon.

Fig. 4.2 shows the configurational density of states for the B_n clusters, $n = 12, 16, 19, 24, 32$. It can be clearly seen that with the increase of the number of atoms as the structural motif of boron system changes from planar to cages, the energy levels in the density of states becomes more and more closely spaced or in other words the system becomes glassy which is clearly seen in case of B_{32} . Similar kind of observations can be made for B_{80} cluster too. In case of B_{80} we started minima hopping run from the previously proposed B_{80} fullerene structure, which consists of the C_{60} fullerene

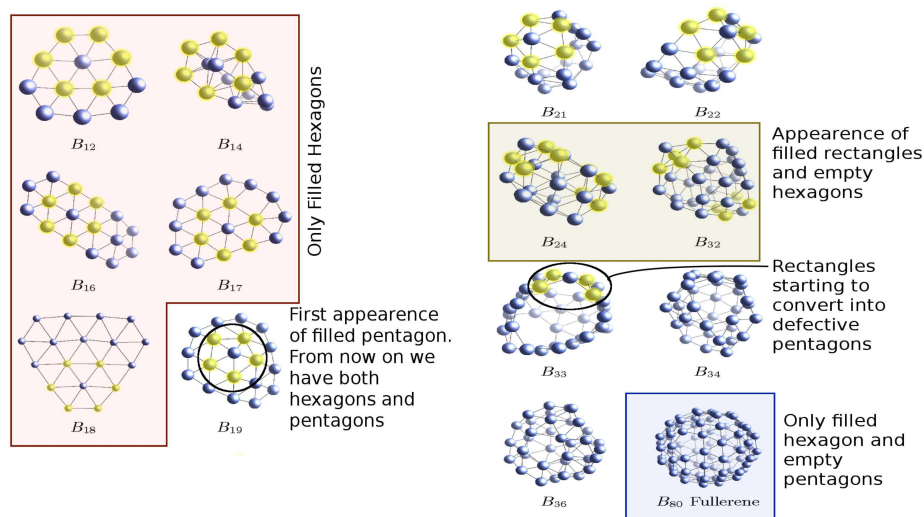


Figure 4.1: Structural evolution of small and medium boron clusters

with 20 additional atoms filled into the hexagons. It thus consists of 20 filled hexagons and 12 empty pentagons. The insertion of the 20 atoms can be viewed as some kind of doping which stabilizes the two-dimensional boron network [18].

During a long period the cage structure was not destroyed in the minima hopping run. Instead minima hopping explored the defect structures that we have described previously [21] as well as other cage structures which are slightly lower in energy than the Szwacki fullerene. Since there is a very large number of possible defect structures this cage funnel contains a very large number of local minima and it takes longer for minima hopping to escape from it.

Once one escapes from the fullerene funnel one finds significantly lower energy structures. These structures contain the icosahedral B_{12} motif which is the basic building block of elemental boron. This icosahedron is in most cases at the base of a dome like structure or otherwise at the center of a spherical cage. Both the domes and the cages consist mainly but not exclusively of

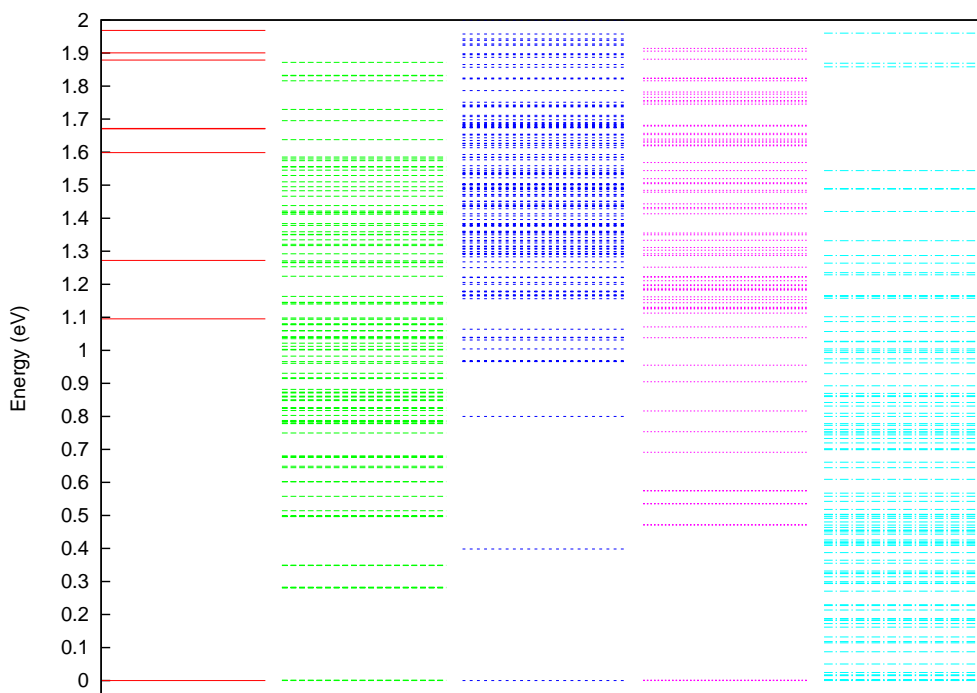


Figure 4.2: Configurational density of states for $n = 12, 16, 19, 24, 32$ left to right

filled and empty hexagons and pentagons.

Fig. 5.5 shows the configurational density of states for the B_{80} cluster. The majority of the structures are of the dome type and the energies of dome type and fullerene type structures overlap. Like for the medium size boron clusters many structural building blocks can be combined to form clusters of very similar energy. Hence the energy difference between the low energy isomers is again very small. The lowest energy structure we found is considerably lower in energy than the recently proposed compact B_{80} structure [9], both within the LDA and PBE functionals.

In addition to the B_{80} cluster we also examined the B_{92} and B_{100} cluster. A structure with a icosahedron in the center of a 80 atom Szwacki fullerene is 7.8 eV lower than the fullerene which was obtained by filling the 12 pentagons [6] shown in fig. 4.6. The resulting structure has however not anymore a high symmetry. A stuffed fullerene structure was proposed for

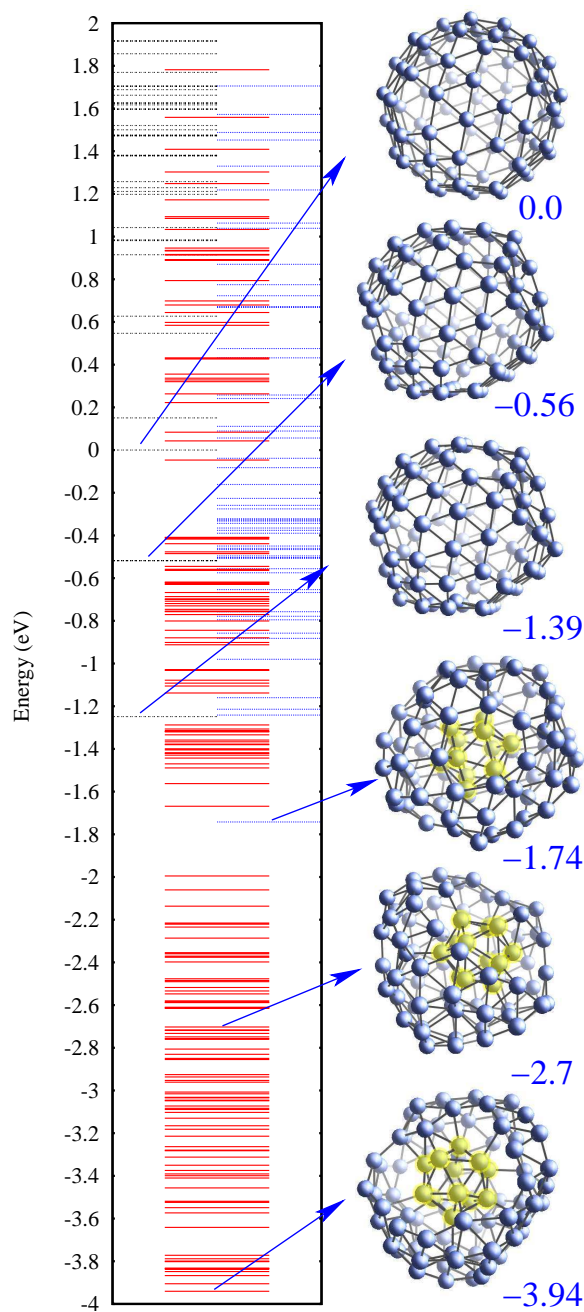


Figure 4.3: The configurational energy spectrum of B_{80} . The energy of the Szwacki fullerene is taken to be zero. The energy levels of the icosahedron-dome structures are centered whereas the levels shifted to the left are fullerene like structures. The levels on the right correspond to centered icosahedron structures. The atoms of the icosahedron are shown in yellow. The structure at an energy of -2.7 eV is the putative global minimum from ref [9]. The energy per atom of our lowest energy B_{80} structure is about .13 eV per atom higher in energy than the sheet structure of Tang and Ismail-Beigi [18].

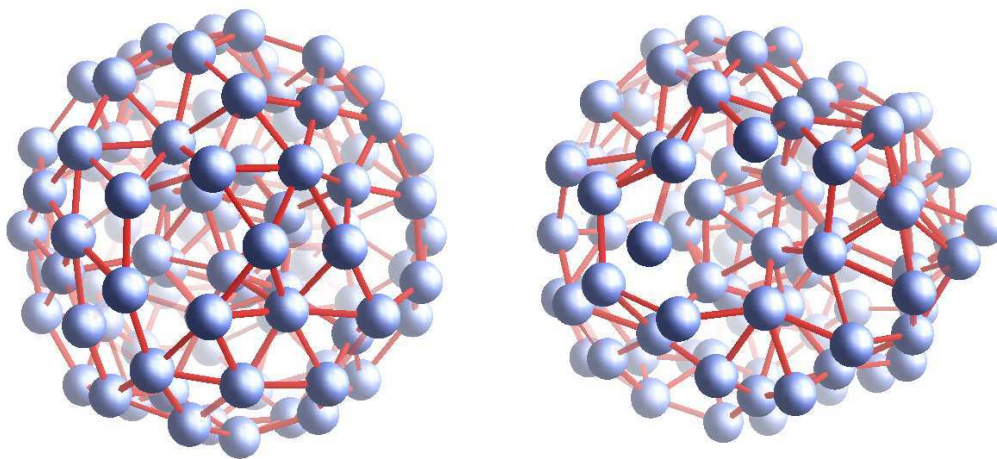


Figure 4.4: Starting from a high symmetry B_{92} cluster (a) minima hopping found a low symmetry structure (b) which is lower in energy by 1.47 eV

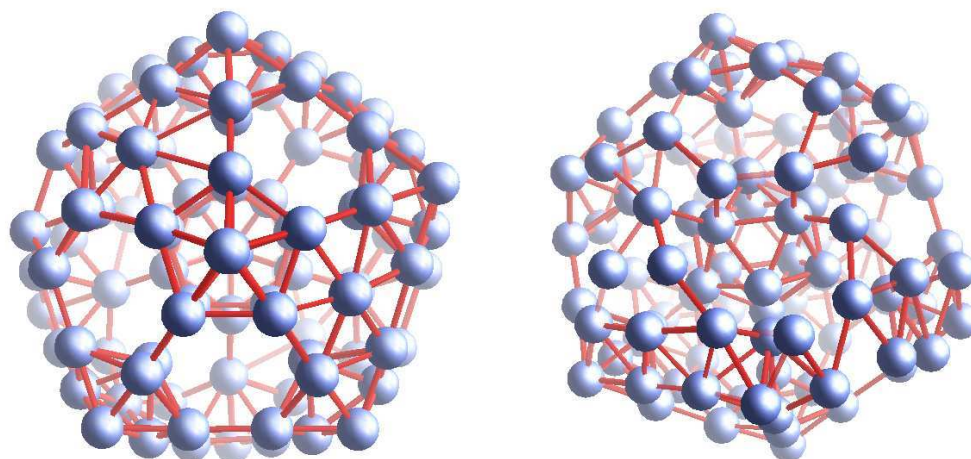
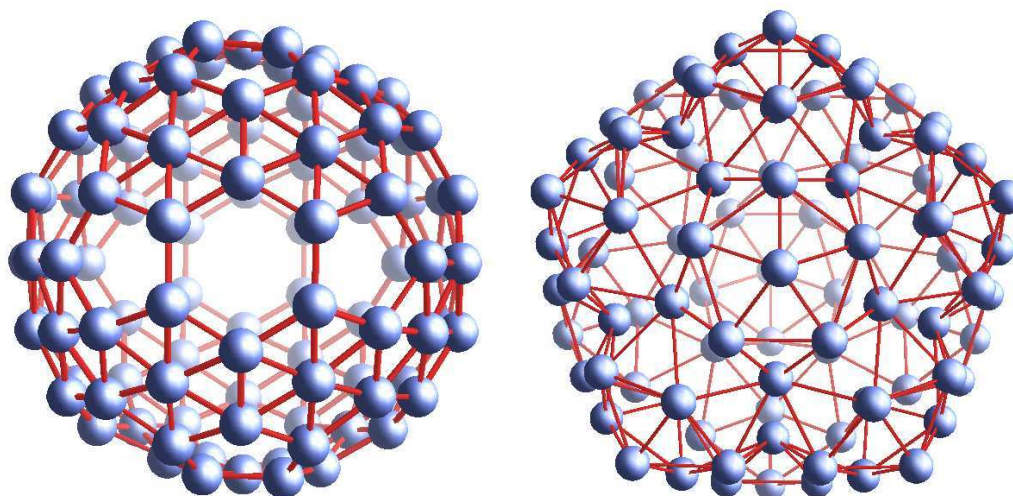


Figure 4.5: Starting from a high symmetry B_{100} cluster [25] (a) minima hopping found a low symmetry structure (b) which is lower in energy by 3.61 eV



(a) B_{100} fullerene proposed by bostani [26] (b) A highly symmetric B_{92} fullerene is 9.8 eV higher in energy than the global minimum obtained by MHM
 is 9.8 eV higher in energy than the global minimum obtained by MHM
 A highly symmetric B_{92} fullerene obtained by filling all the pentagons and hexagons of C_{60} fullerene is 7.8 eV higher in energy than the global minimum obtained by MHM

Figure 4.6: B_{100} and B_{92} fullerenes

B_{100} [25]. Doing minima hopping runs starting from this configuration some structures with lower energy and lower symmetry were found as well. These structures were also about 10 eV lower in energy than the recently proposed B_{100} fullerene [26], shown in fig. 4.6.

These results show that disordered cages with an icosahedron inside are the basic structural motif for boron clusters in this size range. Among all the ground state structures of boron clusters of any size, we could not find any high symmetries. Hence the vibrational modes have no or only low degeneracy. Fig 4.4 shows a highly symmetric metastable structure of B_{92} which is 2.47 eV higher in energy than the global minimum found for the system which no longer possesses any symmetry. The similar observation can also be made in case of B_{100} clusters. Fig 4.5 shows a highly symmetric structure, starting from which minima hopping found another low symmetry structure which is lower in energy by 3.61 eV.

§4.3 Chemical bonding in boron

The conventional bonding concepts that are central to carbon compounds, do not hold in the case of boron. Boron exhibits sp^2 hybridization in most of its compounds, leaving one unhybridized p orbital unoccupied. In this bonding picture, boron has more bonding orbitals than available electrons, so it is considered "electron deficient". Boron adapts by adopting a multi-centered bonding strategy that involves sharing electrons across BBB units, which necessitates formation of cluster compounds. For all types of planar cluster systems, stabilization is not always achieved solely by delocalized σ electrons. There can also be a contribution from π delocalization of electrons occupying unhybridized p orbitals in the plane of a cyclic structure. Some hydrocarbons and inorganic clusters with fully occupied p and s shells have "double aromaticity," a concept first introduced about 25 years ago by Paul v. R. Schleyer and coworkers.

Boron has three valence electrons and a short covalent radius, undergoing sp^2 hybridization in many boron clusters. That leaves one empty $2p_z$ atomic orbital (AO) and renders boron electron-deficient. Mulliken population analysis showed partial population of such AOs in boron clusters, which occurs through sp -promotion. Consequently, planar boron clusters contain delocalized π systems consisting of such $2p_z$ orbitals. The aromatic character of planar and quasiplanar boron clusters and their molecular ions can be estimated from their topological resonance energy (TRE) [29, 30]. The TRE is defined within the framework of Huckel theory as a difference between the total π -binding energies of a given molecule and the graph theoretical polyene reference. It represents extra thermodynamic stabilization due to cyclic conjugation.

If we consider the α boron sheets proposed by Ismail-Beigi [18] shown in fig 4.7 one can see that each atom has six nearest neighbors but only three valence electrons. No two-center bonding scheme leads to a proper description. The three-center bonding model is essential to describe the bonding in the boron sheet. Fig 4.7 shows a choice of orientations for the sp^2 hybrids where three hybrids overlap within an equilateral triangle formed by three neighboring atoms. For such an isolated triangle, we have a simple 3×3 tight-binding problem with D_3 symmetry. Its eigenstates are dictated by group theory: one low-energy symmetric bonding orbital b and two de-

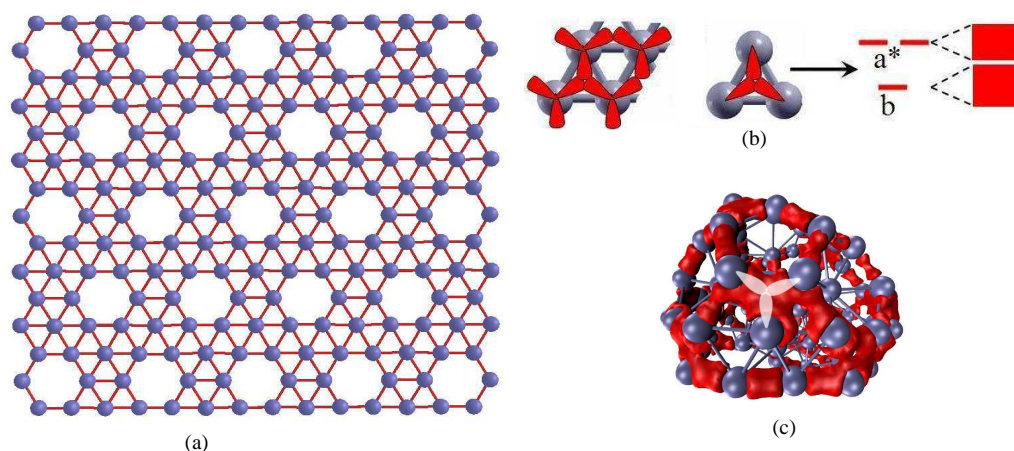


Figure 4.7: (a) Boron alpha-sheet (b) Three-center bonding scheme in flat triangular sheets. Left: orientation of sp^2 hybrids. Center and right: overlapping hybrids within a triangle (D_3 symmetry) yield one bonding (b) and two anti-bonding (a^*) orbitals. These then broaden into bands due to inter-triangle interactions. The p_z orbitals are not shown here. (c) Example of three-center bonding in case of B_{80} global minimum.

generate high-energy antibonding orbitals a^* . (This is closed three-center bonding). Separately, the p_z orbitals also broaden (not shown in the fig 4.7) into a single band. Ideally this sheet would be most stable if

1. two electrons per atom would completely fill the b -derived inplane bonding bands,
2. the antibonding a^* -derived bands were empty, and
3. the remaining electron per atom would half fill the low-energy (bonding) portion of the p_z -derived band.

the most stable α sheet satisfies these condition precisely.

In case of cage like structures also similar bonding nature exists. There exist both two center and three center bonds in case for boron clusters. This three center bonding model was also used to explain the extreme theoretical stability of B_{80} fullerenes, which is composed of triangular motifs with pentagonal holes. It was argued that the stability is due to a balance of two- and three-center bonds. The α sheet was also considered the precursor of B_{80} just as graphene is the precursor of carbon fullerenes [18].

§4.4 Conclusion

In this chapter global minima of several boron clusters were presented. The configurational energy spectrum gives an idea about the nature of the energy landscape for such clusters. For medium and large boron cages the energy landscape is glassy which is a characteristic of amorphous materials. The knowledge of boron clusters gathered in this chapter will be used to develop a methodology to comment on experimental feasibility of synthesis of boron fullerene cages which has been proposed repeatedly by theoreticians yet experimentalists failed to synthesize them until now.

References

- [1] Kagaku, Vol. 25, p.854 (1970) ; Thrower, P. A.(1999). "Editorial". Carbon 37: 16771678
- [2] Kroto et al. (1985). . Nature 318: 162163.
- [3] E. Spano et al., J. Phys. Chem. B 2003, 107, 10337; B. Wang et al., J. Phys. Chem. C 2010, 114, 5741 ; T. Oku et al., Chemical Physics Letters 380 (2003) 620; Phys. Rev. Lett. 87, 045503 (2001) V. Kumar et al. Phys. Rev. Lett. 88, 235504 (2002) V. Kumar et al. Phys. Rev. Lett. 90, 055502 (2003) V. Kumar et al. Nano Lett. 4, 677 (2004). V. Kumar et al. Phys. Rev. B72, 125427 (2005) Young-Cho Bae et al Phys. Rev. B79, 085423 (2009), V. Kumar J. U. Reveles et al. PNAS December 5, 2006 vol. 103 no. 49 18405-18410 J. Ulises Reveles et al. ,J. Phys. Chem. C 2010, 114, 1073910744 Satya Bulusu et al. PNAS May 30, 2006 vol. 103 no. 22 8326-8330 Johansson M. P. et al. (2004) Angew. Chem. Int. Ed 43:26782681 M. Walter et al. , Phys. Chem. Chem. Phys. 2006 P. Pochet et al., Rev. B 82, 035431 (2010).
- [4] A. Willand et al, Phys. Rev. B **81**, 201405(R) (2010)
- [5] Szwacki et al., Phys. Rev. Lett. 98, 166804 (2007)
- [6] R. Zope, Europ. Phys. Lett. 85 68005-p1 (2009) ; N. G. Szwacki, Nanoscale Res. Lett. 3, 49 (2008).
- [7] D. L. V. K. Prasad and E. D. Jemmis, Phys. Rev. Lett. 100, 165504 (2008)

-
- [8] Jijun Zhao, Lu Wang, Fengyu Li, and Zhongfang Chen *J. Phys. Chem. A*, 2010, 114 (37), pp 99699972
- [9] S. Goedecker, *J. Chem. Phys.* **120**, 9911 (2004); S. Goedecker, W. Hellmann, and T. Lenosky, *Phys. Rev. Lett.* **95**, 055501 (2005).
- [10] L. Genovese *et al.*, *J. Chem. Phys.* **129**, 014109 (2008).
- [11] S. Goedecker, M. Teter, and J. Hutter, *Phys. Rev. B* **54**, 1703 (1996).
- [12] J. Perdew, K. Burke, and M. Ernzerhof, *Phys. Rev. Lett.* **77**, 3865 (1996).
- [13] Zhi Xu, Dmitri Golberg, Yoshio Bando *Chemical Physics Letters* 480, 110 (2009)
- [14] Yafei Li *et al.*, *J. of Chem. Phys.*, 130, 204706 (2009)
- [15] L. Wang, J. Zhao, F. li and Z. Chen, *Chem. Phys. Lett.* 501, 16 (2010)
- [16] I. Boustani, *Phys. Rev. B* 55, 16426 (1997)
- [17] H. Tang and S. Ismail-Beigi, *Phys. Rev. Lett.* 99, 115501 (2007)
- [18] Dodecahedrane Robert J. Ternansky, Douglas W. Balogh, and Leo A. Paquette *J. Am. Chem. Soc.*; 1982; 104(16) pp 4503 - 4504
- [19] Leo A. Paquette, Robert J. Ternansky, Douglas W. Balogh, and Gary Kentgen (1983). "Total synthesis of dodecahedrane". *Journal of the American Chemical Society* 105 (16): 54465450
- [20] Pochet *et al.*, *Phys. Rev. B* 83, 081403(R) (2011)
- [21] A. Stone and D. Wales, *Chem. Phys. Lett.* **128** 501 (1986)
- [22] Fabio Pietrucci and Wanda Andreoni, *Phys. Rev. Lett.* 107, 085504 (2011)
- [23] A. Oganov *et al.*, *Nature* 457 863 (2009)
- [24] Prasad *et al.* ,*Phys. Rev. Lett.* 100,165504 (2008)
- [25] C. Özdoğan, S. Mukhopadhyay, M. Hayami, Z. Güvenc, R. Pandey, and I. Boustani , *J. Phys. Chem. C* 114, 4362 (2010)

-
- [26] D. Wales, *Science* 293 page 2067 2001
- [27] A. Heuer, *Journal of Physics: Condensed Matter* 20, 373101 (2008) ; G. Daldoss, O. Pilla, G. Vilianni, C. Brangian and G. Ruocco, *Phys. Rev. B* **60** 3200 (1999)
- [28] Aihara, J. J. *Phys. Chem. A* 2001, 105, 5486.
- [29] Aihara, J. J. *Am. Chem. Soc.* 1976, 98, 2750. Gutman, I.; Milun, M.; Trinajstić, N. *J. Am. Chem. Soc.* 1977, 99, 1692. Aihara, J. J. *Am. Chem. Soc.* 1977, 99, 2048. Aihara, J. *Pure Appl. Chem.* 1982, 54, 1115.

Energy Landscapes Of Fullerene Materials

§5.1 Introduction

Hundreds of new nano-structures have been proposed based on theoretical calculations while only a tiny fraction of them could be synthesized experimentally. The theoretical predictions are generally based on the criteria of zero force on each atom and an imaginary phonon frequency of the proposed system. It is well known that these criteria only indicate that the proposed structure is a local minimum in the energy landscape of the system. But the proposed structure also has to be the global minimum of the system in order to exist in nature. Because of the difficulties faced in global geometry optimizations, finding global minimum of a given system is not a easy job. The problem becomes more and more complicated and difficult to handle with increase of number of atom in the system. Here we present a methodology which can comment on the experimental feasibility of a proposed cluster in small to medium size range. We have taken fullerene cages as an example to describe the method.

§5.2 Fullerene Cages

A fullerene is any molecule composed generally of carbon atoms in the form of a hollow sphere, ellipsoid or tube. Spherical fullerenes are also called

Bucky-balls, and they resemble the football in an atomic scale. Cylindrical ones are called carbon nanotubes or buckytubes. Fullerenes are similar in structure to graphite, which is composed of stacked graphene sheets of linked hexagonal rings; but they may also contain pentagonal (or sometimes heptagonal) rings.

The first fullerene to be discovered, buckminsterfullerene (C_{60}), was prepared in 1985 by Richard Smalley, Robert Curl, James Heath, Sean O'Brien, and Harold Kroto at Rice University. The name was an homage to Buckminster Fuller, to whose geodesic domes it resembles. The structure was also identified some five years earlier by Sumio Iijima, from an electron microscope image, where it formed the core of a "bucky onion." Fullerenes have since been found to occur in nature. In mathematical terms, the structure of a fullerene is a trivalent convex polyhedron with pentagonal and hexagonal faces. In graph theory, the term fullerene refers to any 3-regular, planar graph with all faces having 5 or 6 vertices. It follows from Euler's polyhedron formula, $V - E + F = 2$ (where V, E, F are the numbers of vertices, edges, and faces), that there are exactly 12 pentagons in a fullerene and $V/2 - 10$ hexagons.

The experimental synthesis of fullerenes is a very difficult task. The carbon fullerene structures were therefore theoretically predicted [1] long before they could be produced in the lab [2]. Many more hollow and endohedrally doped fullerene structures made out of elements different from carbon have also been proposed since then theoretically [3] in searches of other possible building blocks for nano-sciences. The similarities between B-N and C-C bonds made boron and nitrogen natural candidates to form fullerene and nanotube structures. Indeed, a method to synthesize pure boron nitride nanotubes was reported in 1995 by N. G. Chopra [4]. Several $(BN)_x$ fullerene structures were predicted. Among them $B_{16}N_{16}$ has been found specially stable. Recently $B_{16}N_{16}$ has also been found short lived in experiments.

It is however surprising that since the experimental discovery of the carbon fullerenes some 25 years ago no other stable fullerenes have been synthesized. So the question is whether experimentalists have just not yet found a way to synthesize these theoretically predicted fullerenes, or whether they do not exist at all in nature. In our group we have recently found [5] that all the theoretically proposed endohedral Si_{20} fullerenes are meta-stable and can thus most likely not be found in nature. In this chapter we investigate in detail boron clusters.

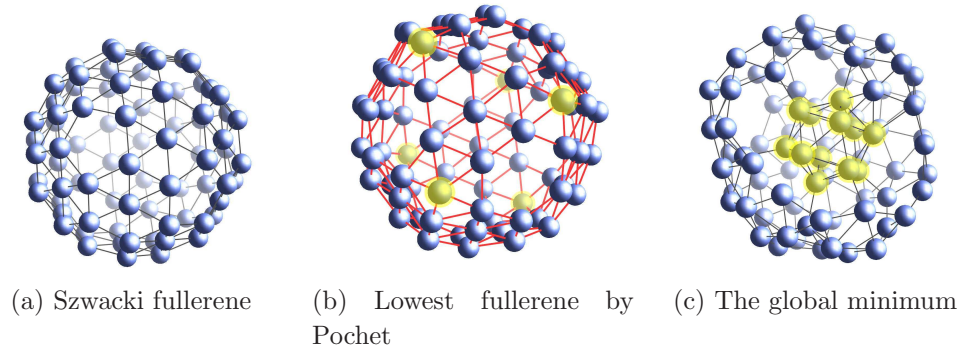
§5.3 Boron Fullerene

The most promising candidate among the proposed boron fullerene family is B_{80} fullerene. Following the B_{80} fullerene structure proposed by Szwacki et al. [6] various other fullerene [7] and stuffed fullerene structures [8] were proposed. Subsequently it was however shown for B_{80} that there exist non-fullerene structures [9] which are lower in energy. We will contrast the characteristics of the potential energy landscape (PES) of these boron clusters with those of systems found in nature, namely carbon and boron nitride fullerenes and find that there are important differences.

In order to explore the energy landscape, we did global geometry optimization runs for the B_{80} cluster. A first run started from the Szwacki fullerene, which consists of the C_{60} fullerene with 20 additional atoms filled into the hexagons. It thus consists of 20 filled hexagons and 12 empty pentagons as shown in Fig 5.1a . The insertion of the 20 atoms can be viewed as some kind of doping which stabilizes the two-dimensional boron network [18]. During a long period the cage structure was not destroyed in the minima hopping run. Instead minima hopping explored the defect structures where instead of all filled hexagon and empty pentagons there exist several structures having few filled pentagons too [21]. We found other cage structures which are slightly lower in energy than the Szwacki fullerene.

The lowest local minimum in this structural motif was found to be a defect structure which contains 6 filled pentagons and 14 filled hexagons. The structure found to be 10.2 meV per atom lower in energy than previously proposed Szwacki fullerene. Fig 5.1b shows this structure where the 6 atoms in the middle of the pentagons have been highlighted. Since there is a very large number of possible defect structures this cage funnel contains a very large number of local minima and it takes long time for minima hopping to escape from it.

Once one escapes from the fullerene funnel one finds significantly lower energy structures. These structures contain the icosahedral B_{12} motif which is the basic building block of elemental boron. This icosahedron is in most cases at the base of a dome like structure or otherwise at the center of a spher-

Figure 5.1: B_{80} clusters

ical cage. Both the domes and the cages consist mainly but not exclusively of filled and empty hexagons and pentagons. Fig. 5.5 shows the configurational density of states for the B_{80} cluster. The energy of the Szwacki fullerene is taken to be zero. The energy levels of the icosahedron-dome structures are centered whereas the levels shifted to the left are fullerene like structures. The levels on the right correspond to centered icosahedron structures. The atoms of the icosahedron are shown in yellow. The structure with an energy of -2.7 eV is the putative global minimum from ref [9]. The energy per atom of our lowest energy B_{80} structure is about 0.13 eV per atom higher in energy than the sheet structure of Tang and Ismail-Beigi [18]. The majority of the structures are of the dome type and the energies of dome type and fullerene type structures overlap. Like for the medium size boron clusters many structural building blocks can be combined to form clusters of very similar energy. Hence the energy difference between the low energy isomers is again very small. The lowest energy structure we found is considerably lower in energy than the recently proposed compact B_{80} structure [9], both within the LDA and PBE functionals. The Global minimum is shown in fig. 5.1c where there is a perfect icosahedron at one side of the the cluster and the other atoms forms a hemispherical bowl like cap on it. The icosahedron has been highlighted in the figure.

§5.4 Fullerenes in Nature

After we have explored the energy landscape of the proposed boron fullerene, we study the energy landscape of a few fullerenes made of other materials

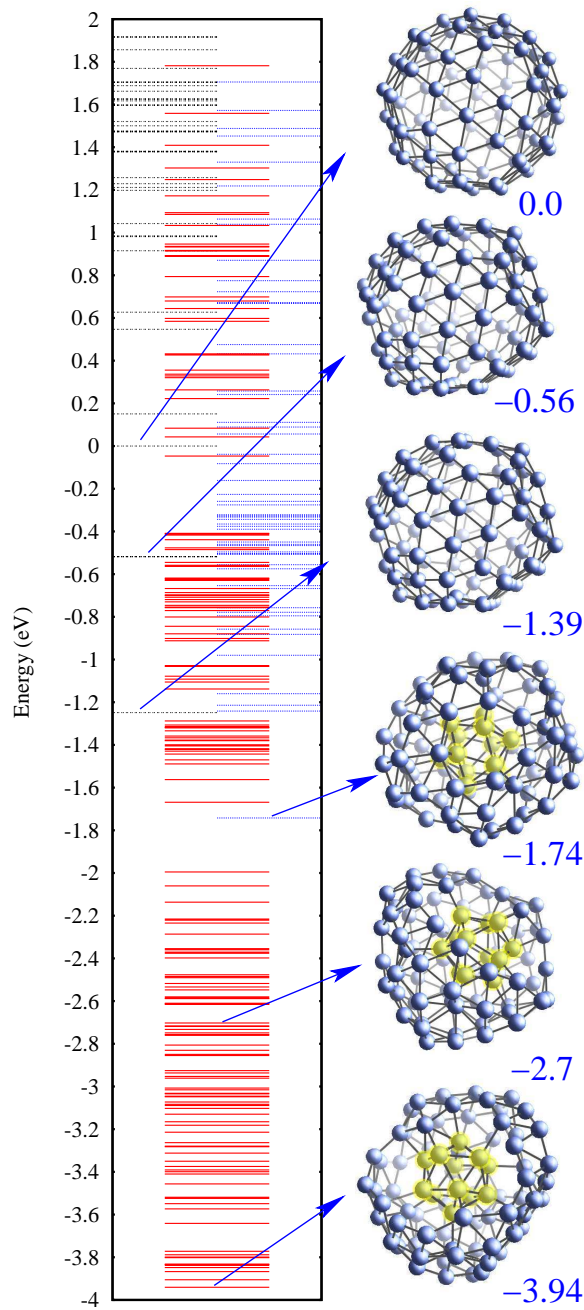


Figure 5.2: The configurational energy spectrum of B_{80} . The energy of the Szwacki fullerene is taken to be zero. The energy levels of the icosahedron-dome structures are centered whereas the levels shifted to the left are fullerene like structures. The levels on the right correspond to centered icosahedron structures. The atoms of the icosahedron are shown in yellow. The structure at an energy of -2.7 eV is the putative global minimum from ref [9]. The energy per atom of our lowest energy B_{80} structure is about .13 eV per atom higher in energy than the sheet structure of Tang and Ismail-Beigi [18].

which are already found in nature. The most obvious candidate for this, is C_{60} fullerene. In addition to C_{60} , we did the similar study on $B_{16}N_{16}$ and $C_{20}H_{20}$.

5.4.1 C_{60} Fullerenes

For C_{60} the first meta-stable structure is a Stone-Wales [22] point defect which is nearly 1.6 eV higher in energy than the fullerene ground state. In the stone-Wales defect there are two pentagons adjacent to each other, where as in case of the perfect fullerene no two pentagons are adjacent to each other. Various defects can be combined to form cages of higher and higher energy. Fig. 5.3 shows the energy spectrum of C_{60} fullerene. Three lowest energy isomer and two high energy isomers are also presented in the figure. One can see that the energy levels are well separated in energy. Two high energy structures are shown in Fig. 5.4. The lowest non-cage like structures are however some 30 eV higher in energy than the ground state and there exists cage structures which are even higher than 30 eV. This shows that in contrast to B_{80} the cage like and non-cage like structures are widely separated in energy. There is consequently a strong driving force towards cage like structures and finding the ground state for C_{60} is much easier than for B_{80} .

The differences in the potential energy landscape between B_{80} and C_{60} are also well illustrated by the following computer experiment. If one does a local geometry optimization for 80 boron atoms starting from random positions one obtains disordered structures which are already fairly low in energy, namely about 10 eV higher than the ground state. This is in contrast to the case of 60 carbon atoms where a local geometry optimization starting from random positions gives structures which are about 50 eV above the ground state unless they happen to be cage like. Fig 5.4 shows two high energy cage like structure for C_{60} fullerene. This shows again that the boron potential energy landscape has a glassy character with a lot of disordered low energy structures. The energy landscape of C_{60} on the other hand has a broad and deep funnel which leads to the ground state fullerene.

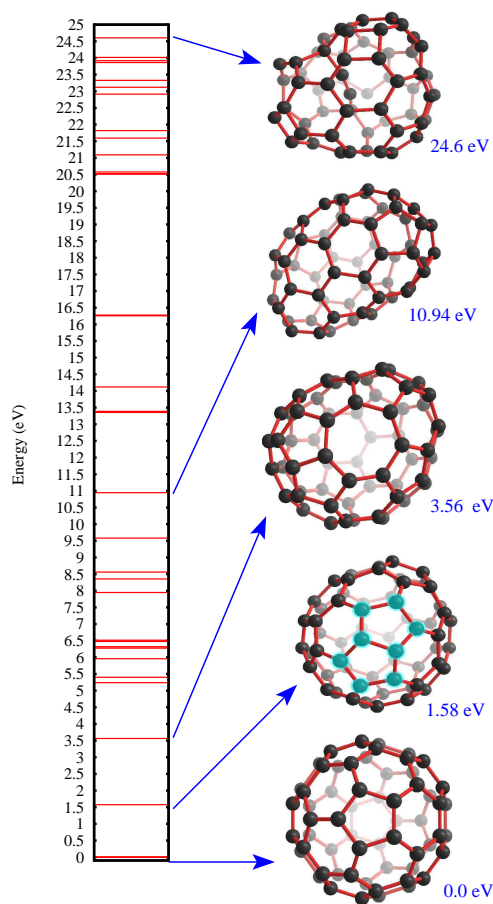
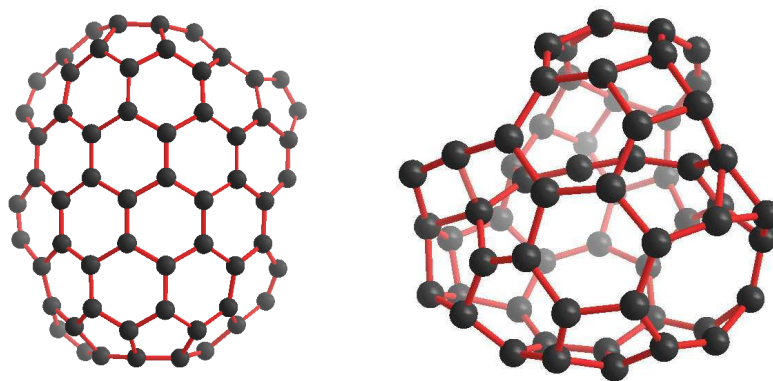


Figure 5.3: The energy spectrum of C_{60} fullerene. For a energy range of almost 25 ev there exist cage like structures. The local minima are well separated in energy and the first metastable structure known as Stone-Wales [22] point defect which is 1.58 eV higher in energy than the fullerene ground state. The presence of two adjacent pentagons has been highlighted in case of the Stone-Wales defect [22]. In the given energy range all the clusters are cage like. Structures that are even higher in energy can possess some chains with 2-fold coordination and anchor atoms for these chains with 4-fold coordination. The structure on the top is an example of such a cage and is 24.6 eV higher than the ground state.



(a) Lowest non cage structure for C_{60} (30.8 eV)

(b) A high energy cage structure for C_{60} (36.3 eV)

Figure 5.4: Two high energy C_{60} cluster.

5.4.2 Boron-Nitride Fullerene

Next, we start out by analyzing the $B_{16}N_{16}$ cluster which was found to be short lived in experiments [14]. In this system structural rigidity is imposed by a strong preference for sp² hybridization [15] as well as by the requirement that bonds are only formed between atoms of different type. This leads to a small configurational density of states.

As shown in Fig. 5.5 there exists a fairly large energy interval in which only cage like structures exist. Hence there is a strong driving force towards the ground state cage structure and minima hopping can find it rapidly. This driving force also allows the formation of $B_{16}N_{16}$ in nature. In the figure boron atoms are shown in blue and nitrogen atoms in red. The higher energy cage structures can be described as a ‘basket’ with a ‘handle’ made out of a chain of 4 atoms (two of each type). Similar to C_{60} energy landscape here also one can see that there is a distinct energy gap of nearly 0.7 eV between global minimum and first metastable structure and analogous to C_{60} here is also a strong driving force to form cage structures.

5.5 $C_{20}H_{20}$: A stable dodecahedrane found in nature

$C_{20}H_{20}$ was first synthesized by Leo Paquette of Ohio State University in 1982, primarily for the “aesthetically pleasing symmetry of the dodecahedral framework”. [19] [20] In this molecule, each vertex is a carbon atom that bonds to three neighboring carbon atoms. The 108° angle of each regular pentagon is close to the ideal bond angle of 109.5° for an sp³ hybridized atom. Each carbon atom is bonded to a hydrogen atom as well. The molecule, like fullerene, has Ih symmetry, evidenced by its proton NMR spectrum in which all hydrogen atoms appear at a single chemical shift of 3.38 ppm. $C_{20}H_{20}$ is a very stable chemical compound and that’s why we also studied the energy landscape properties of this system. There exist very few metastable structures for the system and they are widely spaced in energy. Fig 5.6 shows the energy levels and structures of 1st five low energy isomers. One can see the energy gap between global minimum and first local minimum in this case is more than 2 eV. The nature of the landscape is again similar to C_{60} and $B_{16}N_{16}$ and represents a deep funnel like energy landscape which can be used to explain the stability of the system.

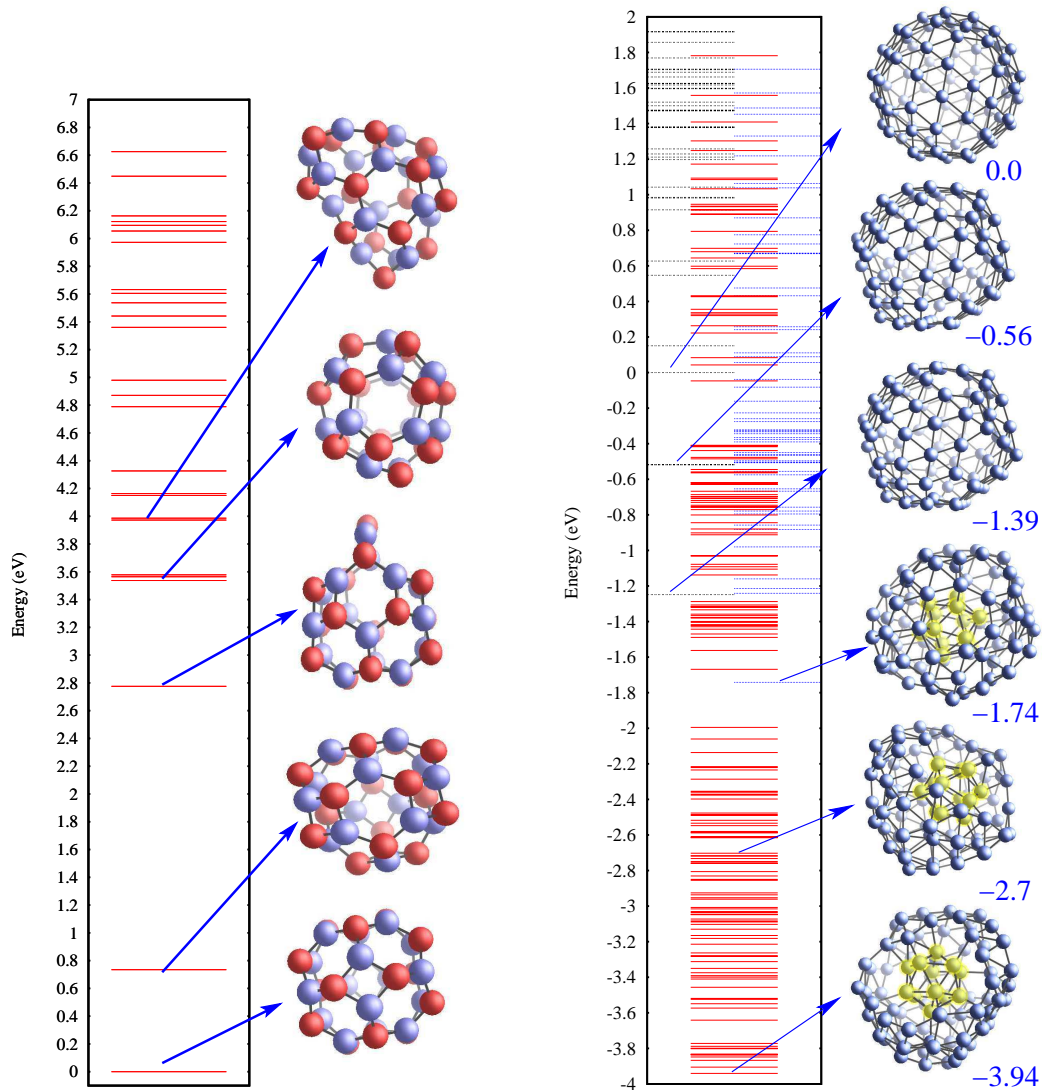
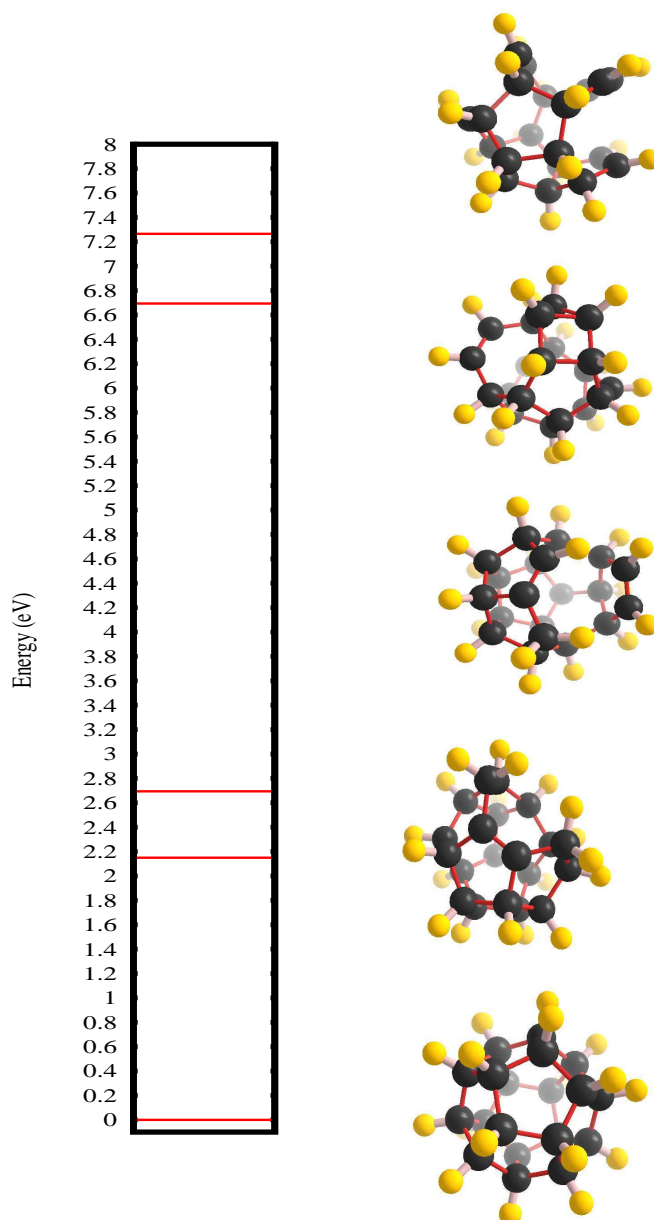


Figure 5.5: a) The configurational energy spectrum of $B_{16}N_{16}$. (b) The configurational energy spectrum of B_{80} .

§5.6 Comparison of energy landscapes

From Fig 5.3 and Fig 5.5 we can clearly see that the energy landscape of B_{80} is completely different than that of C_{60} and $B_{16}N_{16}$. The energy levels in case of B_{80} is very closely spaced and there exists many defect structures which have very similar energy values. This kind of energy landscape is a

Figure 5.6: The energy spectrum of $C_{20}H_{20}$. The energy levels are widely spaced. There exist a large gap of 2.14 eV between global minimum and first metastable structure. The structures corresponding to global minimum and first four local minima are also presented on the right side.



distinct signature of glassy energy landscape. It is also very clear that in finite temperature B_{80} system will consist of these defect structures along with the global minimum of the system. On the other hand the large energy gap between global minimum and first local minimum in case of both C_{60} and $B_{16}N_{16}$ fullerene indicates the non-glassy nature of the landscape and makes them suitable for experimental synthesis.

5.6.1 Fingerprint Vector

As discussed earlier, because of amorphous and glassy nature of boron energy landscapes there exists many local minima which visually looks very similar and are closely spaced in energy where on the other hand in case of C_{60} or boron-nitride system a small defect causes a large energy separation between two structures. We wanted to show this contradiction more clearly using mathematical tools. For this purpose we calculated ‘‘Finger print’’ vectors of each local minimum obtained by Minima-Hopping for B_{80} , C_{60} and $B_{16}N_{16}$ following the method described in the paper by Fabio Pietrucci and Wanda Andreoni [23].

In order to calculate the finger print vectors we consider a matrix based on a function of distance between each pair of atom (r_{ij}). The elements of the matrix $[a_{ij}]$ is defined by

$$a_{ij} = \frac{1 - (r_{ij}/r_0)^m}{1 - (r_{ij}/r_0)^n}$$

where r_0 is the bondlength of the system and n, m are the intergers whose value depends on the system ($n > m$). $[a_{ij}]$ is symmetric, non-negative, and also irreducible when it represents a connected graph (the cluster), i.e., if any pair of vertices is connected through a path. In this case the Perron-Frobenius theorem holds: The largest modulus eigenvalue λ^{max} is real, positive, and non-degenerate, and the corresponding eigenvector v_i^{max} has all nonzero components with equal sign. We adopt the positive sign convention. In particular, a few very interesting properties can be shown:

1. λ^{max} carries global information on the network: It grows with the number of bonds and lies between the average and the maximum coordination number (CN)

2. v_i^{max} carries information about both the short and long-range topology of the atomic network surrounding atom i : For any positive integer M ,

$$v_i^{max} = \frac{1}{(\lambda^{max})^M} \sum_j a_{ij}^M v_j^{max}$$

where a_{ij}^M is the number of walks of length M connecting i and j . Above equation shows the “social character of v_i^{max} ”.

These observations suggest to combine the largest eigenvalue and corresponding eigenvector into the definition of fingerprint vector (\vec{FP}). The components of the \vec{FP} is given as

$$FP_i = \sqrt{N} \lambda^{max} v_i^{max,sorted}; \quad i = 1, 2, \dots, N$$

where N is the number of atoms and the i th component must be taken after sorting the eigenvector from its smallest to its largest component. It is this sorting operation that makes the set FP_i invariant with respect to the $N!$ permutations of the labeling of N identical atoms (and thus also with respect to point-group symmetries).

After calculating finger print vector for all the local minima obtained in a minima hopping run, we define the finger print distance F_d as

$$F_d(\text{localminimum}) = |\vec{FP}_{\text{localminimum}} - \vec{FP}_{\text{globalminimum}}|$$

This parameter gives an rough idea of how different the local minimum is from the global minimum of the system.

In fig 5.7 we plot energy per atom relative to ground state vs fingerprint distance F_d for the three systems together. Higher value of fingerprint distance implies more difference in the structure of the local minimum than the global minimum. The blue, black and red indicates B_{80} , C_{60} and $B_{16}N_{16}$ systems respectively. In the figure one can see that for B_{80} there exists many structures which have similar energy values but have very different fingerprint distances. This indicates that even if the clusters look very different, they can have similar energy. This kind of behaviour is clearly opposite of that of carbon and boron-nitride systems where a small difference in fingerprint distance causes a high change in energy values.

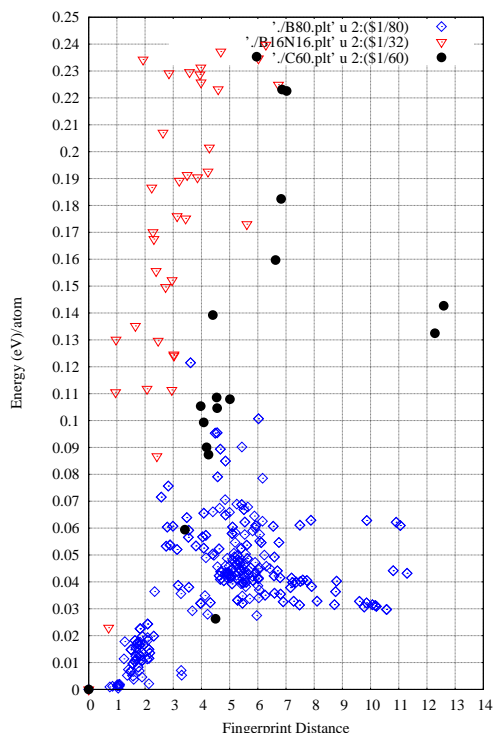


Figure 5.7: Energy per atom relative to ground state vs fingerprint distance F_d for B_{80} (blue), C_{60} (black) and $B_{16}N_{16}$ (red). Higher values of the fingerprint distance imply larger differences in the structure of the local minima compared to the global minimum. One can see that for B_{80} there exists many structures which have similar energy values but have very different fingerprint distances. This indicates that even if the clusters look very different, they can have similar energy. This kind of behaviour is clearly opposite of that of carbon and boron-nitride systems where a small difference in fingerprint distance causes a high change in energy values.

§5.7 Cluster Interactions

After we present the difference in energy landscapes of the proposed boron cluster with that of the fullerenes found in nature, next we wanted to see how the boron clusters interact with each other. For this purpose we placed the two clusters close to each other at a distance comparable to the bondlength of the system and did a local geometry optimization. Fig 5.8 shows the interaction between the global minimum of B_{80} , the proposed perfect fullerene structure and another smaller B_{32} cage. Fig. 5.9 shows the interaction between two and three cluster having high symmetry. The two clusters are found heavily interacting, resulting a combined structure which is 8 eV lower in energy. For three interacting clusters, it was found that the interaction between one pair is stronger than the interaction between another pair and the resulting system is 15 eV lower in energy than the isolated starting configuration. In all cases we found that the boron clusters prefer to stick together and make a bigger clusters rather than retaining their structural motif. This behavior is also in contrast to that of boron nitride and carbon fullerene. As shown in fig 5.10 $B_{16}N_{16}$ found to be repulsive to each other where as

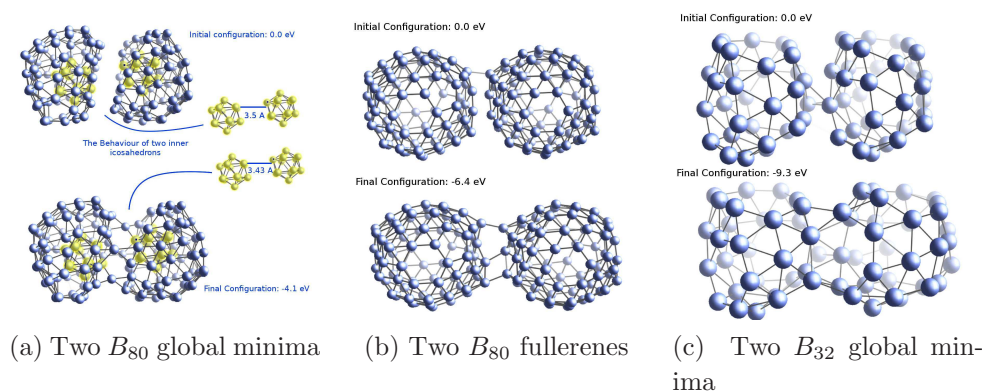
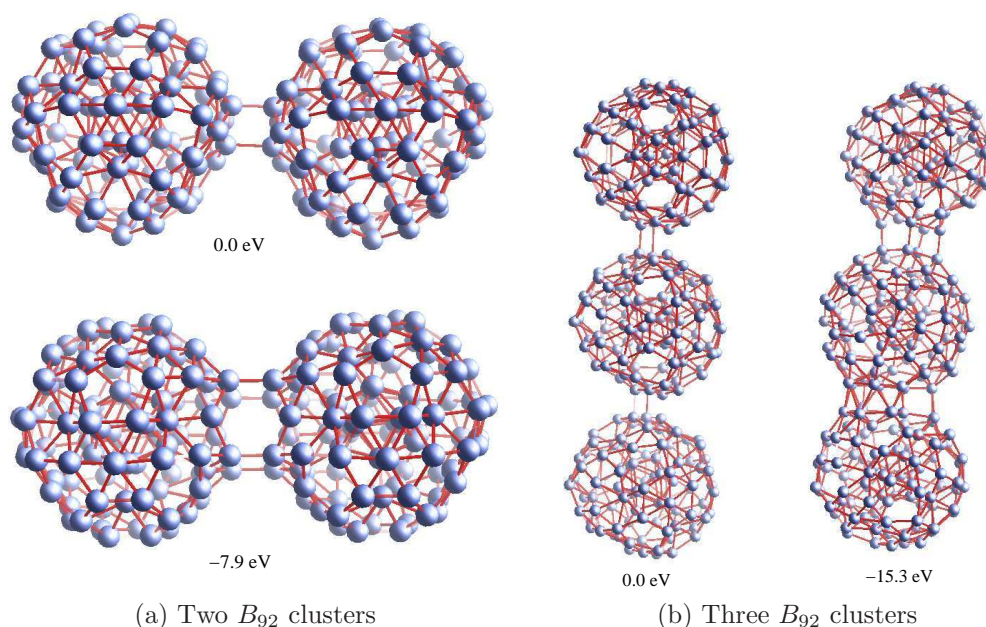


Figure 5.8: The interaction between boron clusters

Figure 5.9: The interaction between B_{92} clusters

C_{60} fullerenes are very weakly interacting. In both cases they retain their structural motif and do not get destroyed upon contact like boron cages. We also observe an interesting phenomenon in case of the interaction between two B_{80} global minima in fig 5.8. One can see that although the two clusters come close and stick with each other the inner icosahedra do not get distorted at all. This shows that the icosahedron is very stable. This is not surprising as they are, a matter of fact, the building block of bulk boron

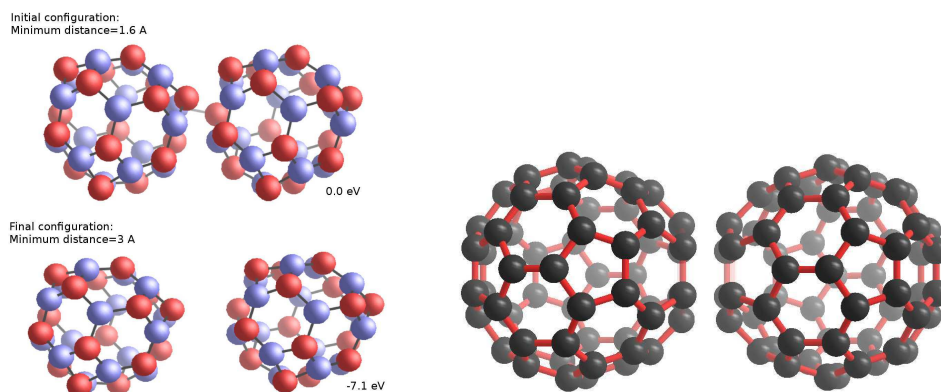


Figure 5.10: The interaction between two $B_{16}N_{16}$ and two C_{60}

system (See fig 5.11). So the interaction also gives an indication that upon contact to a large number of similar structures the system will try to form the bulk system rather than retaining their structural motif in isolation.

Among all the ground state structures of boron clusters of any size, we could not find any high symmetries. Hence the vibrational modes have no or only low degeneracy. Employing some mode following method will therefore in general lead to different transition states with different barrier heights. Since the height of the barrier correlates with curvature along the starting mode [27], one can expect for a cluster of low symmetry a broader distribution of barrier heights and therefore a larger probability of finding low energy barriers [28]. If low barriers exist a small modification of the external environment such as the presence of another cluster can make these barriers disappear. Hence it is not surprising that all boron structures that we examined, independently of whether they are medium size, large, cage-like or not, turned out to be chemically reactive with other boron clusters when they are brought into contact. During such a chemical reaction with another cluster several chemical bonds are formed which leads to a considerable lowering of the energy and to a large distortion or even destruction of the original structures. This means that even though medium size clusters have a strong tendency for cage formation in isolation, it is unlikely that such boron cages exist in nature. This behavior is also in contrast to the behavior of the C_{60} and $B_{16}N_{16}$ fullerenes. They are only weakly interacting and do not form chemical bonds when they are brought into contact. The chemical reactivity

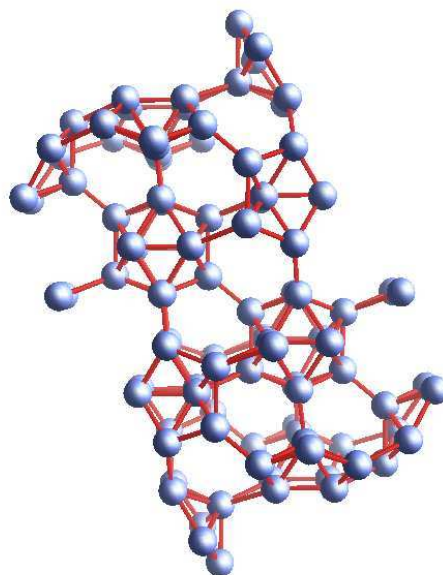


Figure 5.11: The structure of a simple rhombohedral form of bulk boron is based on icosahedra

of the boron clusters can also be rationalized in a local picture. If many different structural motifs can be used as a building block of a low symmetry cluster, it is very likely that some atoms have some dangling bonds which are chemically reactive.

§5.8 Conclusion

Our results explain why boron fullerenes have not been found experimentally. Boron clusters are frustrated systems which do not have enough electrons to fill all electronic orbitals in a chemical bonding based on pure sp^2 hybridization and they consequently do not exhibit some clear preference for a simple structural motif. Hence, from an energetical perspective, there is no driving force towards some well defined structure. Instead one finds a glassy energy landscape with a large number of different low energy structures whose energies are very similar. These structures are chemically reactive and will therefore not be found under experimental conditions.

The glassy energy landscape of bulk boron has been explained by the frustrated bonding features of boron where 2-center bonds have to coexist with 3-center bonds [24]. The glassy energy landscape of the medium size boron clusters can also be explained in this way. Fig. 5.12 shows the co-

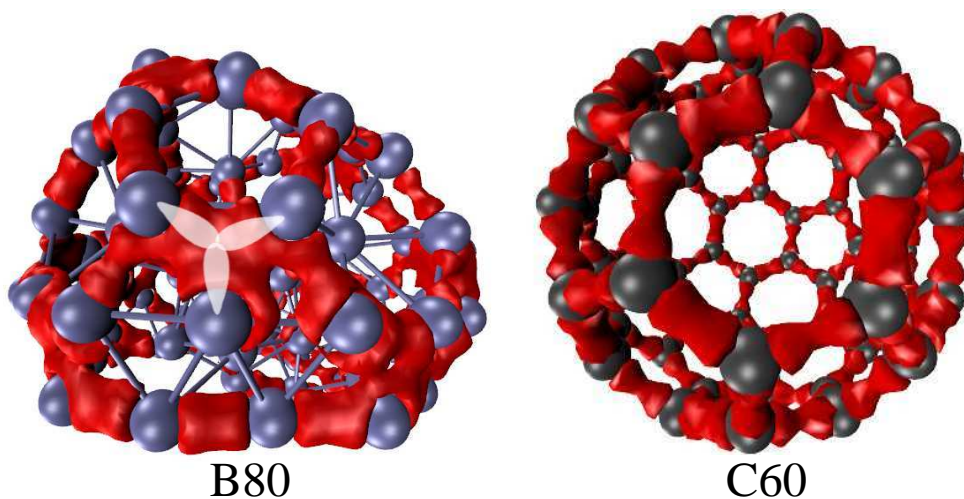


Figure 5.12: The iso-surfaces of the valence charge density in our lowest B_{80} cluster and the C_{60} fullerene. They are evaluated at 70% of the maximum value (0.12 a.u. respectively 0.24 a.u.). Whereas in C_{60} we see only two center bonds, both 2 and 3 center bonds are visible in B_{80} .

existence of these two types of bonds in our lowest energy B_{80} . The fact that no elemental boron but only compounds containing boron can be found on earth however indicates the possibility of synthesizing more complicated boron cages such as metal doped boron fullerenes.

Such a doping can energetically pull down the cage like part of the configurational space of boron clusters [21].

Our simulations demonstrate that one can make theoretical predictions about the feasibility of an experimental synthesis. In order to judge whether a system can be formed in nature, it is not necessary to simulate its synthesis process explicitly by molecular dynamics or similar methods.

A global geometry optimization with the Minima Hopping algorithm indicates whether the system being simulated is a structure seeker or a system with a glass like potential energy surface. For a glassy system finding the global minimum is slow because one has to explore energetic regions with a large density of minima whose energies are very similar. For a structure seeker on the other hand the energy goes down rapidly and by significant amounts as one approaches the ground state. Only for these latter systems it is to be expected that synthesis pathways can be found.

Our work thus clearly shows that theoretical cluster structure prediction has to be based on global geometry optimization because only this approach gives the necessary information on the potential energy landscape. The standard approach based on structures, obtained from educated guesses, that were subsequently locally relaxed, gives only a very incomplete characterization of a system. A ground state structure predicted by global geometry optimization has a reasonable chance of being found in nature in significant quantities only if,

- The global minimum is at the bottom of a broad and deep funnel
- The global minimum is significantly lower in energy than the other low energy meta-stable structures and
- The global minimum has high symmetry.

References

- [1] Kagaku, Vol. 25, p.854 (1970) ; Thrower, P. A. (1999). "Editorial". Carbon 37: 16771678
- [2] Kroto et al. (1985). . Nature 318: 162163.
- [3] E. Spano et al., J. Phys. Chem. B 2003, 107, 10337; B. Wang et al., J. Phys. Chem. C 2010, 114, 5741 ; T. Oku et al., Chemical Physics Letters 380 (2003) 620; Phys. Rev. Lett. 87, 045503 (2001) V. Kumar et al. Phys. Rev. Lett. 88, 235504 (2002) V. Kumar et al. Phys. Rev. Lett. 90, 055502 (2003) V. Kumar et al. Nano Lett. 4, 677 (2004). V. Kumar et al. Phys. Rev. B72, 125427 (2005) Young-Cho Bae et al Phys. Rev. B79, 085423 (2009), V. Kumar J. U. Reveles et al. PNAS December 5, 2006 vol. 103 no. 49 18405-18410 J. Ulises Reveles et al. ,J. Phys. Chem. C 2010, 114, 1073910744 Satya Bulusu et al. PNAS May 30, 2006 vol. 103 no. 22 8326-8330 Johansson M. P. et al. (2004) Angew. Chem. Int. Ed 43:26782681 M. Walter et al. , Phys. Chem. Chem. Phys. 2006 P. Pochet et al., Rev. B 82, 035431 (2010).
- [4] N.G. chopra et al Science 269,966
- [5] A. Willand et al, Phys. Rev. B **81**, 201405(R) (2010)
- [6] Szwacki et al., Phys. Rev. Lett. 98, 166804 (2007)
- [7] R. Zope, Europ. Phys. Lett. 85 68005-p1 (2009) ; N. G. Szwacki, Nanoscale Res. Lett. 3, 49 (2008).

-
- [8] D. L. V. K. Prasad and E. D. Jemmis, Phys. Rev. Lett. 100, 165504 (2008)
- [9] Jijun Zhao, Lu Wang, Fengyu Li, and Zhongfang Chen J. Phys. Chem. A, 2010, 114 (37), pp 99699972
- [10] S. Goedecker, J. Chem. Phys. **120**, 9911 (2004); S. Goedecker, W. Hellmann, and T. Lenosky, Phys. Rev. Lett. **95**, 055501 (2005).
- [11] L. Genovese *et al.*, J. Chem. Phys. **129**, 014109 (2008).
- [12] S. Goedecker, M. Teter, and J. Hutter, Phys. Rev. B **54**, 1703 (1996).
- [13] J. Perdew, K. Burke, and M. Ernzerhof, Phys. Rev. Lett. **77**, 3865 (1996).
- [14] Zhi Xu, Dmitri Golberg, Yoshio Bando Chemical Physics Letters 480, 110 (2009)
- [15] Yafei Li et al., J. of Chem. Phys., 130, 204706 (2009)
- [16] L. Wang, J, Zhao, F. li and Z. Chen, Chem. Phys. Lett. 501, 16 (2010)
- [17] I. Boustani, Phys. Rev. B 55, 16426 (1997)
- [18] H. Tang and S. Ismail-Beigi, Phys. Rev. Lett. 99, 115501 (2007)
- [19] Dodecahedrane Robert J. Ternansky, Douglas W. Balogh, and Leo A. Paquette J. Am. Chem. Soc.; 1982; 104(16) pp 4503 - 4504
- [20] Leo A. Paquette, Robert J. Ternansky, Douglas W. Balogh, and Gary Kentgen (1983). "Total synthesis of dodecahedrane". Journal of the American Chemical Society 105 (16): 54465450
- [21] Pochet et al., Phys. Rev. B 83, 081403(R) (2011)
- [22] A. Stone and D. Wales, Chem. Phys. Lett. **128** 501 (1986)
- [23] Fabio Pietrucci and Wanda Andreoni, Phys. Rev. Lett. 107, 085504 (2011)
- [24] A. Oganov et al., Nature 457 863 (2009)
- [25] Prasad et al. ,Phys. Rev. Lett. 100,165504 (2008)

-
- [26] C. Özdoğan, S. Mukhopadhyay, M. Hayami, Z. Güvenç, R. Pandey, and I. Boustani, *J. Phys. Chem. C* 114, 4362 (2010)
- [27] D. Wales, *Science* 293 page 2067 2001
- [28] A. Heuer, *Journal of Physics: Condensed Matter* 20, 373101 (2008) ; G. Daldoss, O. Pilla, G. Vilianni, C. Brangian and G. Ruocco, *Phys. Rev. B* **60** 3200 (1999)
- [29] Aihara, J. *J. Phys. Chem. A* 2001, 105, 5486.
- [30] Aihara, J. *J. Am. Chem. Soc.* 1976, 98, 2750. Gutman, I.; Milun, M.; Trinajstić, N. *J. Am. Chem. Soc.* 1977, 99, 1692. Aihara, J. *J. Am. Chem. Soc.* 1977, 99, 2048. Aihara, J. *Pure Appl. Chem.* 1982, 54, 1115.

6

Conclusions and Outlook

The energy landscapes of atomic clusters made of several elements has been explored using Minima Hopping Method and many new global minima has been presented in this dissertation. The work also addresses the importance and difficulties associated with the prediction of the global minimum of atomic clusters. In chapter one we have introduced the basic concept of the potential energy landscape and discussed why global minima structures play an important role in physics, chemistry and biology. We also introduced the basic terms and definitions required to describe the energy landscape in general. We discussed the difficulties associated with the exploration of the PES and pointed out the fact that except for few systems, e.g. C_{60} , $C_{20}H_{20}$, $B_{16}N_{16}$ etc, having simple funnel like landscape, most of the clusters have energy landscapes containing multiple funnels and large number of closely spaced local minima, which makes it extremely difficult to find global minima.

In chapter two we discussed several important global optimization methods. We discussed the advantages and drawbacks of a few important methods in this field and pointed out why the Minima Hopping method is well suited for the kind of systems we are interested in. Our problems require energy and force evaluation within the density functional theory framework which is very expensive even for modern supercomputers. Minima hopping algorithm was previously coupled with the Bigdft program and optimized to a great extent, which made the work possible, presented in this dissertation.

In the second part of the thesis, we discussed the results of our studies.

In chapter three we addressed a basic question, " Are the global minima of charged and neutral clusters related ?" To find the answer to this question we considered two systems namely, silicon clusters as representatives of semiconductor materials and magnesium clusters as representatives of metallic clusters. In contrast to the usual assumption and belief, we came to the conclusion that the global minima of charged and neutral systems are in general not related and can in fact be quite different. This study was first of its kind and we reached the conclusion that there is no reason to assume that the global minima of charged and neutral system will be same unless the global minima contain some high symmetry and the energy gap between the global minimum and the first local minimum is large. A example of such a system would be the C_{60} fullerene.

From the fourth chapter on we started discussing boron clusters. We discussed how the structural motif evolves when the number of atoms in the system increases. It was shown that small boron clusters prefer planar structure whereas medium and large clusters prefer to form cages. From the data we gathered, it was evident that with the increase of size, the energy landscapes of boron clusters become more and more glassy, which makes it very difficult to explore in order to find the global minimum. Nevertheless, Minima Hopping succeeds in finding putative global minima structures for several boron clusters, among which B_{80} was the most notable one. For B_{80} we reported a new global minimum which is almost 4 eV lower in energy than the previously reported perfect fullerene structure.

In the fifth chapter we discussed the energy landscapes of fullerene materials. Since the discovery of the C_{60} fullerene, scientists are trying to synthesize fullerene cages made of elements other than carbon. The fullerene structures are of great importance in terms of both practical uses and theoretical studies. Several fullerene cages made of non carbon elements, mostly boron and nitrogen have been proposed by theoreticians. In spite of the huge number of theoretically proposed structures, it is surprising to know that even after discovery of the C_{60} fullerene almost 25 years ago, till date only a few stable fullerene cages made of other elements ($(ZnO)_{60}$ [1], $(MgO)_{12}$ [2], $(MoS_2)_n$, $(WS_2)_n$ [3] etc) could be synthesized successfully by the experimentalists. The B_{80} fullerene cage was the most promising candidate in the line. After we established the fact that the perfect fullerene cage was not the

global minimum for the B_{80} cluster, we studied the differences of the energy landscape of B_{80} with a few other fullerene cages found in nature. The differences were very prominent which led us to develop a methodology which can comment on the feasibility of experimental synthesis of a proposed nano structure.

The Minima Hopping Method turns out to be a very powerful tool in the field of structure prediction of clusters. It could not only predict the global minima of a variety of systems, but it also provided valuable information on the energy landscape of the system. Several clusters made of other elements which were not reported here were also studied and MHM could find the global minima in all cases. Some of the works were done in collaboration with other groups and some of them will be used for future publications. Fig 6.1 indicates the elements we studied. At this point we did not want to unnecessarily lengthen the thesis by putting the data of large number of global minima, without any physical interpretation, so we decided to build a cluster database, which will be useful for future studies.

The work presented here goes beyond the mere prediction of new stable clusters. We addressed few basic questions, which are independent of the global optimization methods used or the global minima found. The fact that there is no theoretical criterion which would allow to distinguish the global minimum from all local minima, implies that there is always a possibility that in future new global minima could be discovered, especially for the big systems we studied. Considering this fact, we gave more importance towards the basic understanding of the energy landscapes, rather than only focussing on the prediction of new structures. The obtained result lead us to comment on basic questions such as the relation of the charged and neutral global minima or the feasibility of experimental synthesis of a theoretically proposed cluster. We hope that the original work presented here will stimulate new studies in the field of structure prediction, which will be able to guide the experimentalists much better than at present for new discoveries of nano systems.

References

- [1] Baolin Wang, Xiaoqiu Wang and Jijun Zhao, Atomic Structure of the Magic (ZnO)₆₀ Cluster: First-Principles Prediction of a Sodalite Motif for ZnO Nanoclusters, *J. Phys. Chem. C* 2010, 114, 57415744
- [2] Marko Haertelt, Andre Fielicke, Gerard Meijer, Karolina Kwapien, Marek Sierkaz and Joachim Sauerb; Structure determination of neutral MgO clusters-hexagonal nanotubes and cages; *Phys. Chem. Chem. Phys.*, 2012, 14, 28492856
- [3] Inorganic Fullerene-Like MS₂ (M=Mo,W) Structures: Synthesis, Reaction mechanism and Characterization, G.L. Frey, Y. Feldman, M. Homyonfer, V. Lakhovitskaya, G. Hodes, and R. Tenne, 11th International Winter School on Electronic Properties of Novel materials, Kirchberg, March (1996).
Inorganic Fullerene-Like Materials and Nanotubes, R. Tenne, *Chem. Isr.* 1, 5 (1999)
Inorganic Fullerenes, R. Tenne and L. Margulis, *The Isr. Chemist* 14, 60 (1995).

List Of Publications

1. **Sandip De**, Alexander Willand, Maximilian Amsler, Pascal Pochet, Luigi Genovese, and Stefan Goedecker: Energy Landscape of Fullerene Materials: A Comparison of Boron to Boron Nitride and Carbon, **Phys. Rev. Lett.** **106**, 225502 (2011) [\[link\]](#)
2. **Sandip De**, S. Alireza Ghasemi, Alexander Willand, Luigi Genovese, Dilip Kanhere, and Stefan Goedecker: The effect of ionization on the global minima of small and medium sized silicon and magnesium clusters, **J. Chem. Phys.** **134**, 124302 (2011)[\[link\]](#)
3. Seyed Mohammad Ghazi,**Sandip De**, D. G. Kanhere, and Stefan Goedecker : Density functional investigations on structural and electronic properties of sodium clusters Na_N (N=40-147): Comparison with the experimental Photoelectron spectra,**J. Phys.: Condens. Matter** **23** 405303[\[link\]](#)
4. Heidari, Ideh; **Sandip De**; Ghazi, Seyed Mohammad; Goedecker, Stefan; Kanhere, D.G. : Growth and Structural Properties of Mg_N (N=10-56) Clusters: Density Functional Theory Study”,**J. Phys. Chem. A** **2011**, **115**, **12307** **12314** [\[link\]](#)
5. Pascal Pochet, Luigi Genovese, **Sandip De**, Stefan Goedecker, Damien Caliste, S. Alireza Ghasemi, Kuo Bao, and Thierry Deutsch: Low-energy boron fullerenes: Role of disorder and potential synthesis pathways, **Phys. Rev. B** **83**, 081403(R) (2011) [\[link\]](#)

Sandip De

Curriculum Vitae

Contact Information Department of physics
University of Basel
Klingelbergstrasse 82
Basel 4056, Switzerland

Office: +41 61 267 3910
Mobile: +41 78 878 5036
E-mail: sandip.de@unibas.ch

Date of Birth 22nd April 1986

Academic	2009-2012	PhD in Theoretical Physics	University of Basel, Basel, Switzerland
	2007-2009	M.Sc Physics	University of Pune, Pune, India
	2004-2007	B.Sc Physics(honours)	St. Xavier's College, kolkata (University of Calcutta), India

Honours and Awards	2009	CSIR-NET Fellowship	Council of Scientific & Industrial Research, India
	2009	Graduate Aptitude Test in Engineering (GATE)	Indian Institute of Technology, India
	2008	Summer Internship program For Indian Students	National University of Singapore, Singapore

Computational Skills

- Bigdft (Extensively)
- Minima hopping (Extensively)

Used Codes

- Abinit
- DLPOLY
- VASP
- GAMESS

Development

- Algorithmic and technical development for BigDFT and Minima-Hopping Codes during My Phd.
- Development of various codes for structural analysis of clusters.
- Development of DFT code for a three dimensional confined electron system from scratch during my M.Sc project.

Programing Languages

- Fortran 77, Fortran 90
- Advanced Shell Scripts
- Basic knowledge of parallel programming language: MPI, OpenMP and CUDA
- Python and Visual Python
- Basic Knowledge of C
- Basic
- LOGO
- L^AT_EX

Conferences And Workshops	2012	APS March Meeting	Boston,USA (Oral Presentation)
	2012	Invited Talk, Hosted by Prof. Dr. Michele Parrinello	Computational Science Department of Chemistry and Applied Biosciences - ETH Zurich Link
	2012	Invited Talk	ICTP, Trieste,Italy Link
	2011	Conference on Computational Physics (CCP)	Gatlinburg, Tennessee, USA (Oral Presentation)
	2011	Daubechies Wavelets in Electronic Structure Calculation: BigDFT Code Tutorial	Grenoble,France (Tutorial Presentation on Minima Hopping method Link)
	2010	Psi-K 2010 conference	Berlin, Germany (Poster Presentation)
	2010	Parallel Programming Workshop at CSCS	Swiss national super-computing Centre,Manno,Switzerland
	2010	39th SPEEDUP Workshop on High-Performance Computing: Parallel software environments and fault tolerance	ETH Zurich, Switzerland
	2010	38th SPEEDUP Workshop on High-Performance Computing: Multi-core computing and Parallel Languages	EPFL, Laussane, Switzerland
	2010	CAMD Summer School 2010 on the Electronic Structure theory & Materials Design	Department of Physics, DTU, Denmark (Poster Presentation)
	2010	International workshop on frontiers in Electronic structure calculation: Techniques and applications	University of Pune, Pune, India
	2009	Raman Memorial Conference	University of Pune, Pune, India
	2008	Summer Internship program For Indian Students	National University of Singapore, Singapore
	2008	Workshop on low temp physics	Central University of Hyderabad, Hyderabad, India
	2008	Raman Memorial Conference	University of Pune, Pune, India
	2007	Workshop on Space Science & Nano-materials	Kalpana Chawla Space research Centre, Kolkata, India
	2004	Summer School on Basic Sciences for School Leaving Students	Indian Association for the Cultivation of Science, Kolkata, India

**Teaching
Experience**

University of Basel,Basel, Switzerland

Teaching assistant for undergraduate courses in

- Computational Physics
- Statistical Physics

Central University of Rajasthan, Rajasthan, India

- Computational Physics for undergraduate students.